MATHEMATICS OF COMPUTATION
Volume 00, Number 0, Pages 000–000
S 0025-5718(XX)0000-0

AN ENTROPY-STABLE AND FULLY WELL-BALANCED SCHEME FOR THE EULER EQUATIONS WITH GRAVITY

CHRISTOPHE BERTHON, VICTOR MICHEL-DANSAC, AND ANDREA THOMANN

Abstract. The present work concerns the derivation of a first-order numerical scheme to approximate the weak solution of the Euler equations with a gravitational source term. The designed scheme is proved to be fully-well-balanced since it is able to exactly preserve all the moving or at rest stationary solutions. Moreover, the proposed scheme is entropy preserving since it satisfies all the fully discrete entropy inequalities. In addition, in order to satisfy the required admissibility of the approximated solutions, the positivity of both approximated density and pressure are established. Several numerical experiments attest the relevance of the developed numerical method.

1. Introduction

The present paper is devoted to design a numerical scheme to approximate the weak solutions of the well-known Euler equations with a given gravitational source term [19, 32, 42, 31, 36, 39, 40]. From a numerical point of view, such a system poses three main challenges:

- the physical admissibility of the approximated solutions,
- the discrete entropy stability,
- the suitable capture of the steady solutions.

Concerning the admissibility of the discrete solutions; namely to preserve both density and pressure positive, this is the basic property to be satisfied by any first-order numerical scheme. For instance, the Godunov scheme, the HLL and HLLC schemes, the relaxation schemes are usual schemes which satisfy this essential robustness property (see [38, 37, 27, 17, 13, 29] but the list is clearly not exhaustive). However, it is worth noticing that the set made of physically admissible states is not convex so that specific techniques, like entropy inequalities, are required to get a positive approximate pressure law (for instance, see [3]).

Next, the entropy inequalities are essential to rule out some nonphysical solutions. Indeed, since the system under consideration turns out to be of hyperbolic type, discontinuous solutions may be involved [23, 18]. The physical admissibility of the discontinuities are thus governed by the entropy inequalities. The homogeneous Euler system contains a large range of entropy inequalities since they are defined up to a smooth function according to prescribed restrictions [35]. Here, we are concerned by a non-homogeneous Euler system, supplemented by gravitational source term. It is thus very interesting to remark that the gravitational source term

2010 *Mathematics Subject Classification.* Primary .

is compatible with the entropies [19] since it contains the same set of entropy functions than the usual homogeneous Euler system. From a numerical point of view, this essential entropy stability must be preserved. The establishment of discrete entropy inequalities is known to be very challenging for usual homogeneous hyperbolic system. Fro instance, the Godunov scheme, the HLL and HLLC schemes, the Suliciu relaxation scheme, the Xin-Jin relaxation scheme are known are known to be entropy satisfying for Euler equations [23, 13, 9, 3, 19, 27]. Here, we have to deal with additional source terms. In order to recover this crucial stability property, we adopt some recent Godunov-type techniques [33, 4] well-designed to approximate source terms. In particular, in one of our main results, we show that the specific entropy given by the celebrate one intermediate state approximate Riemann solver by Harten, Lax and van Leer [27] satisfies a decreasing principle when convex function composition is applied. This nice and useful principle turns out to be one of our main argument to prove the required discrete entropy inequalities satisfied by the approximate solutions.

The last challenge we have to deal with concerns the accurate capture of the steady solutions. Indeed, because of the source term, the system admits non obvious steady solutions [9, 34, 19]. These particular solutions are of strong interest from a numerical point of view since huge errors can be introduced by the source term discretization and they can be propagate over the whole simulation domain. This numerical failure has been underlined a long time ago in [2, 11, 25, 24] for shallow-water simulations. For over a decade, numerous works have been devoted to the derivation of linear steady states preserving schemes (for instance, see [1, 28, 34, 41, 21, 6]; namely the well-balanced schemes. More recently, the fully-well-balanced schemes were introduced to emphasize the ability of the scheme to exactly restore all steady linear or nonlinear solutions [12, 33, 10, 5, 15, 16, 8]. In this work, according to the Godunov-type scheme to be entropy satisfying, we extend some shallow-water fully-well-balanced schemes to deal with the Euler system endowed with gravitational source terms.

To address these three issues, the paper is organized as follows. In the next section, we introduce the Euler system under consideration and we recall the entropy inequalities satisfied by the weak solutions. We also present the nonlinear steady solutions with non-vanishing velocity. Section 3 is devoted to the derivation of an approximate Riemann solver which must mimic, in a sense to be prescribed, the exact Riemann solution associated to the Euler equations with gravitational source term. This approximate Riemann solver is defined from one hand by the integral consistency condition stated by Harten, Lax and van Leer in [27]. From the other hand, the approximate Riemann solver must be at rest as soon as a steady solution is considered. This condition is a natural way to suitably define the discretization of the source term [5, 33, 7, 22]. Next, we impose the entropy integral consistency condition, stated in [27], to recover the expected discrete entropy inequalities. Equipped with the approximate Riemann solver, we exhibit the associated Godunov-type scheme and we show that the required properties are satisfied: admissibility of the approximated solutions, entropy stability, fully-well-balanced property. In section 4, we adopt a recent technique to increase the order of accuracy of a numerical scheme with fully-well-balanced property [4]. In the next section, we exhibit several numerical experiments to illustrate the relevance of the here designed numerical procedure. A short conclusion is proposed in the last section.

2. The model equations

The goal of this section is to introduce the model under consideration. The Euler equations with gravitational potential are described in Section 2.1. Its steady solutions are then derived, firstly in Section 2.2 with a vanishing velocity and secondly in Section 2.3 with a nonzero velocity.

2.1. The Euler equations with gravity.

We consider the compressible Euler equations, equipped with a gravitational source term and in a one-dimensional setting, governed by

$$\begin{cases} \partial_t \rho + \partial_x(\rho u) = 0, \\ \partial_t(\rho u) + \partial_x(\rho u^2 + p) = -\rho \partial_x \varphi, \\ \partial_t E + \partial_x((E+p)u) = -\rho u \partial_x \varphi, \end{cases} \tag{2.1}$$

where $\rho > 0$ denotes the density, $u \in \mathbb{R}$ the velocity and $E > 0$ the total energy density. Moreover, $\varphi : \mathbb{R} \to \mathbb{R}$ is a given time-independent continuous gravitational potential. The system is closed by the ideal gas equation of state, which defines the pressure $p > 0$ by

$$p = (\gamma - 1)\left(E - \frac{1}{2}\rho u^2\right), \tag{2.2}$$

where $\gamma > 1$ denotes the adiabatic index. To shorten notation, we rewrite system (2.1) in the following compact form

$$\partial_t W + \partial_x(F(W)) = S(W), \tag{2.3}$$

where the state vector W, flux function F and source term S are defined respectively as

$$W = \begin{pmatrix} \rho \\ \rho u \\ E \end{pmatrix}, \quad F(W) = \begin{pmatrix} \rho u \\ \rho u^2 + p \\ u(E+p) \end{pmatrix}, \quad \text{and} \quad S(W) = \begin{pmatrix} 0 \\ -\rho \partial_x \varphi \\ -\rho u \partial_x \varphi \end{pmatrix}.$$

We require the density and pressure to be positive. Thus, the state vector W belongs to the set of admissible states Ω, defined by

$$\Omega = \left\{ W \in \mathbb{R}^3 \ \text{ such that } \ \rho > 0 \text{ and } \ p > 0 \right\}. \tag{2.4}$$

To reflect the influence of the gravitational source term on the wave structure of the Euler equations, we augment system (2.1) by the additional equation $\partial_t \varphi = 0$. The resulting system is hyperbolic with the eigenvalues

$$\lambda_\pm = u \pm c, \quad \lambda_u = u, \quad \lambda_0 = 0,$$

where c denotes the speed of sound, given for the ideal gas law by

$$c = \sqrt{\frac{\gamma p}{\rho}}.$$

This wave structure is represented in the left panel of Figure 1. Note that, compared to the homogeneous system, which is obtained by setting the gravitational source terms in (2.1) to zero, there is a zero eigenvalue associated to the gravitational potential. This leads to a non-ordered wave structure, since $\lambda_\pm$ and λ_u can be positive or negative, depending on the flow. This has a direct consequence on the construction of the Riemann solver, see e.g. [19] where a relaxation model is developed to circumvent the appearance of a zero wave, or [39] where six different cases of wave order configurations had to be taken into account.

Moreover, admissible entropy weak solutions to system (2.1) satisfy the entropy inequality

$$\partial_t(\rho\eta(s)) + \partial_x(\rho u\eta(s)) \leq 0, \tag{2.5}$$

where the specific entropy s is defined by

$$s = -\log\left(\frac{p}{\rho^\gamma}\right). \tag{2.6}$$

After [19], (add refs by tadmor) the entropy function $W \mapsto \rho\eta(s)$ is convex as soon as η is any smooth function satisfying

$$\eta'(s) \geq 0 \quad \text{and} \quad \gamma\eta''(s) + \eta'(s) \geq 0.$$

However, after [], (add refs by maria), the entropy stability of (2.1) is ensured by merely adopting entropies defined by functions η such that

$$\eta'(s) \geq 0 \quad \text{and} \quad \eta''(s) \geq 0. \tag{2.7}$$

Note also that the gravitational source term does not interfere with the definition of the entropy given above. However, the presence of gravity in system (2.1) gives rise to non-trivial steady solutions, which play an important role in many applications. Therefore, Sections 2.2 and 2.3 are devoted to a derivation of the steady solutions of system (2.1).

2.2. **Hydrostatic equilibria.** In this section, we shortly recap some properties of hydrostatic steady states for the Euler equations with gravity. Canceling the time derivatives in (2.1) and setting $u = 0$ shows that hydrostatic steady solutions are characterized by the hydrostatic equation

$$\partial_x p = -\rho\partial_x\varphi. \tag{2.8}$$

Relation (2.8) is the only link between the two unknowns, p and ρ. Thus, hydrostatic equilibria are underdetermined and, to obtain unique solutions of (2.8), additional information about the properties of the equilibrium have to be provided. Intensively studied examples are so-called isothermal hydrostatic equilibria with constant temperature or isentropic hydrostatic equilibria with constant entropy, see e.g. [19, 36, 30, 26]. For example, isentropic hydrostatic equilibria are governed by

$$u = 0, \quad p - \kappa\rho^\gamma = \text{cst}, \quad \text{and} \quad \frac{\kappa\gamma}{\gamma-1}\rho^{\gamma-1} + \varphi = \text{cst}, \tag{2.9}$$

where $\kappa > 0$ is a constant. One can easily check that (2.9) indeed satisfies the hydrostatic equation (2.8).

In this work, we are interested in a more general class of steady states. We discuss below the moving equilibria, where the velocity u is nonzero.

2.3. **Moving equilibria.** Time-invariant solutions of (2.1) with a non-zero velocity $u \neq 0$, the so-called moving equilibria, are governed by the following system

$$\partial_x(\rho u) = 0, \tag{2.10a}$$

$$\partial_x(\rho u^2 + p) = -\rho\,\partial_x\varphi, \tag{2.10b}$$

$$\partial_x((E+p)u) = -\rho u\,\partial_x\varphi. \tag{2.10c}$$

Assuming smooth enough steady states fulfilling (2.10), we obtain from (2.10a) a constant momentum $q_0 = \rho u \neq 0$. Substituting and dividing by q_0 in (2.10c), we find that

$$\frac{E+p}{\rho} + \varphi = H_0, \tag{2.11}$$

where H_0 denotes a constant total enthalpy.

Substituting φ from (2.11) into (2.10b), we obtain

$$\partial_x\left(\frac{q_0^2}{\rho} + p\right) = \rho\,\partial_x\left(\frac{E+p}{\rho}\right) \tag{2.12}$$

Since p is given by (2.2), we note that

$$E + p = \frac{p}{\gamma-1} + \frac{1}{2}\frac{q_0^2}{\rho} + p = \frac{\gamma p}{\gamma-1} + \frac{1}{2}\frac{q_0^2}{\rho}. \tag{2.13}$$

Using the above relation in (2.12) yields

$$-\frac{q_0^2}{\rho^2}\partial_x\rho + \partial_x p = \frac{\gamma}{\gamma-1}\rho\,\partial_x\left(\frac{p}{\rho}\right) + \frac{q_0^2}{2}\rho\,\partial_x\left(\frac{1}{\rho^2}\right).$$

Expanding the derivatives, we obtain

$$-\frac{q_0^2}{\rho^2}\partial_x\rho + \partial_x p = \frac{\gamma}{\gamma-1}\partial_x p - \frac{\gamma}{\gamma-1}\frac{p}{\rho}\partial_x\rho - \frac{q_0^2}{\rho^2}\partial_x\rho.$$

Therefore, multiplying the above relation by ρ and rearranging terms, we get

$$\left(1 - \frac{\gamma}{\gamma-1}\right)\rho\,\partial_x p + \frac{\gamma}{\gamma-1}p\,\partial_x\rho = 0.$$

Since p and ρ are positive, dividing by $p\rho$ and multiplying by $(\gamma-1)$ leads to

$$-\frac{1}{p}\partial_x p + \gamma\frac{1}{\rho}\partial_x\rho = 0,$$

and we obtain

$$\partial_x\big(-\log p + \gamma\log\rho\big) = 0.$$

This immediately leads to

$$\partial_x\left(-\log\left(\frac{p}{\rho^\gamma}\right)\right) = 0,$$

and we recognize the expression of the specific entropy s defined in (2.6). Therefore, smooth moving steady solutions are isentropic, i.e., they satisfy

$$\partial_x s = 0.$$

Hence, smooth moving steady solutions obeying the ideal gas law, with $u \neq 0$, are necessarily isentropic and are characterized by the constant triplet (q_0, H_0, s_0) given by

$$\rho u = q_0, \qquad \frac{E+p}{\rho} + \varphi = H_0, \qquad -\log\left(\frac{p}{\rho^\gamma}\right) = s_0, \tag{2.14}$$

where q_0 is a constant momentum, H_0 is a total enthalpy (including the contribution of the potential energy to the total energy), and s_0 a constant specific entropy.

Remark that, when $q_0 = 0$, moving equilibria immediately reduce to isentropic hydrostatic equilibria, governed by (2.9).

In the following, the objective is to derive a Godunov-type finite volume (FV) scheme based on an approximate Riemann solver (A-RS), which is able to preserve moving equilibria and isentropic hydrostatic equilibria up to machine precision, generates admissible solutions in the sense of (2.4), and fulfills the entropy inequality (2.5).

3. The numerical scheme

We start by briefly recalling the principle of Godunov-type FV schemes based on approximate Riemann solvers. The space domain is discretized, for $i \in \mathbb{Z}$, in uniform cells $C_i = (x_{i-1/2}, x_{i+1/2})$, of center x_i and of size Δx. The time domain is discretized with time steps of varying size Δt. We seek a way to evolve in time an approximation of the solution W to the Euler equations (2.3), defined by

$$W_i^n \simeq \int_{x_{i-\frac{1}{2}}}^{x_{i+\frac{1}{2}}} W(x, t^n)\, dx.$$

To that end, we develop an approximate Riemann solver (A-RS). We first state, in Section 3.1, the structure of our A-RS, as well as the general principle of A-RSs. Then, basic consistency properties are dealt with in Section 3.2, which allows us to define the time evolution of the cell averages, up to the final choice of the A-RS, Section 3.3. The remainder of this section is then devoted to the construction of the remaining parts of the A-RS to achieve some properties given in Section 3.4.

3.1. The approximate Riemann solver.

Let us define an A-RS denoted by $\widetilde{W}$, whose role is to approximate the solution of the Riemann problems occurring at each cell interface. Since this solution is self-similar, the A-RS depends on the variable x/t, as well as the two states left and right of the interface. For instance, the approximate Riemann solution at interface $x_{i+1/2}$ is given by $\widetilde{W}((x - x_{i+1/2})/t; W_i^n, W_{i+1}^n)$.

In this work, we select an A-RS made of two intermediate states, as represented in the right panel of Figure 1. Its expression is given, for two given left and right states W_L and W_R, by

$$\widetilde{W}\left(\frac{x}{t}; W_L, W_R\right) = \begin{cases} W_L & \text{if } x < -\lambda t, \\ W_L^* & \text{if } -\lambda t < x < 0, \\ W_R^* & \text{if } 0 < x < \lambda t, \\ W_R & \text{if } x > \lambda t, \end{cases} \tag{3.1}$$

where the components of the vectors W_L^* and W_R^* are denoted by

$$W_L^* = \begin{pmatrix} \rho_L^* \\ q_L^* \\ E_L^* \end{pmatrix} \qquad \text{and} \qquad W_R^* = \begin{pmatrix} \rho_R^* \\ q_R^* \\ E_R^* \end{pmatrix}.$$

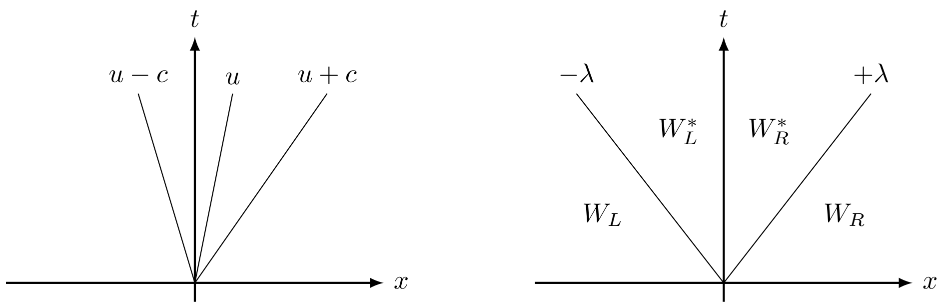

FIGURE 1. Left panel: One possible wave configuration, with $u > 0$, of the Euler equations with gravity (2.1). Right panel: Wave structure of the approximate Riemann solver.

In the A-RS (3.1), the approximate wave speed λ is chosen such that the acoustic waves are included in the wave fan of the A-RS, i.e., $\lambda \geq |u| + c \geq |\lambda_\pm|$. In this work, we impose that the waves defining the A-RS are symmetric around $\lambda_0 = 0$. However, this is just a simplifying assumption. Indeed, in principle, two different values of λ could be chosen, to account for the asymmetric wave configuration of the Euler equations with respect to λ_0, as long the acoustic waves $\lambda_\pm$ are contained in the A-RS. In practice, we take

$$\lambda = \Lambda \max(|u_L| + c(W_L), |u_R| + c(W_R)), \tag{3.2}$$

which indeed satisfies $\lambda \geq |\lambda_\pm|$. The parameter $\Lambda \geq 1$ is merely used to scale the wave speeds, and will be given in the numerical experiments.

The remainder of this section is devoted to the construction of the two intermediate states W_L^* and W_R^*. They will be derived such that the resulting numerical scheme satisfies several key properties, namely consistency, entropy stability (i.e. fulfilling a discrete equivalent of (2.5)), positivity preservation (i.e. $W_i^n \in \Omega$), and well-balancedness. We start with consistency in Section 3.2.

3.2. **Consistency conditions.** Let us first derive conditions on the intermediate states W_L^* and W_R^* to ensure the consistency of the FV scheme with the solution of the Euler system. According to [27], the scheme is consistent as soon as the average over a cell of the A-RS (3.1) is equal to that of the exact, self-similar solution to the Riemann problem, denoted by $W_{\mathcal{R}}$. Therefore, the following equality must hold

$$\frac{1}{\Delta x}\int_{-\Delta x/2}^{\Delta x/2} \widetilde{W}\left(\frac{x}{\Delta t}; W_L, W_R\right) dx = \frac{1}{\Delta x}\int_{-\Delta x/2}^{\Delta x/2} W_{\mathcal{R}}\left(\frac{x}{\Delta t}; W_L, W_R\right) dx. \tag{3.3}$$

Straightforward computations, detailed in [33], then show that the intermediate states must satisfy the following relations:

$$
\begin{cases}
\rho_L^* + \rho_R^* = 2\rho_{\mathrm{HLL}}, \\
q_L^* + q_R^* = 2q_{\mathrm{HLL}} + \dfrac{1}{\lambda\Delta t}\displaystyle\int_{-\Delta x/2}^{\Delta x/2}\int_0^{\Delta t} (-\rho\partial_x\varphi)_{\mathcal{R}}\left(\frac{x}{t}; W_L, W_R\right) dt dx, \\
E_L^* + E_R^* = 2E_{\mathrm{HLL}} + \dfrac{1}{\lambda\Delta t}\displaystyle\int_{-\Delta x/2}^{\Delta x/2}\int_0^{\Delta t} (-q\partial_x\varphi)_{\mathcal{R}}\left(\frac{x}{t}; W_L, W_R\right) dt dx,
\end{cases}
\tag{3.4}
$$

where $(-\rho\partial_x\varphi)_{\mathcal{R}}$ and $(-q\partial_x\varphi)_{\mathcal{R}}$ respectively represent the second and third components of $S(W_{\mathcal{R}})$. Moreover, we have introduced in (3.4) the intermediate state W_{HLL} of the well-known HLL Riemann solver from Harten, Lax and van Leer, described in [27]. It is given by

$$
W_{\mathrm{HLL}} = \begin{pmatrix} \rho_{\mathrm{HLL}} \\ q_{\mathrm{HLL}} \\ E_{\mathrm{HLL}} \end{pmatrix} = \frac{W_L + W_R}{2} - \frac{F(W_R) - F(W_L)}{2\lambda}.
\tag{3.5}
$$

Next, we introduce two new quantities, S^q and S^E, which are approximations of the cell averages of the integrals of the second and third components of the source term, i.e.,

$$
\begin{aligned}
S^q &\approx \frac{1}{\Delta t}\frac{1}{\Delta x}\int_{-\Delta x/2}^{\Delta x/2}\int_0^{\Delta t} (-\rho\partial_x\varphi)_{\mathcal{R}}\left(\frac{x}{t}; W_L, W_R\right) dt dx, \\
S^E &\approx \frac{1}{\Delta t}\frac{1}{\Delta x}\int_{-\Delta x/2}^{\Delta x/2}\int_0^{\Delta t} (-q\partial_x\varphi)_{\mathcal{R}}\left(\frac{x}{t}; W_L, W_R\right) dt dx,
\end{aligned}
\tag{3.6}
$$

where S^q and S^E have to be consistent with $-\rho\partial_x\varphi$ and $-q\partial_x\varphi$, in a sense that will be prescribed later. Then, using relations (3.6) in the consistency condition (3.4) yields the following consistency constraints to be satisfied by the intermediate states

$$
\begin{cases}
\rho_L^* + \rho_R^* = 2\rho_{\mathrm{HLL}}, \\
q_L^* + q_R^* = 2q_{\mathrm{HLL}} + \dfrac{S^q\Delta x}{\lambda}, \\
E_L^* + E_R^* = 2E_{\mathrm{HLL}} + \dfrac{S^E\Delta x}{\lambda}.
\end{cases}
\tag{3.7}
$$

To simplify computations in the following steps, let us introduce $\widehat{W}$ and δW, defined such that

$$
\widehat{W} = \frac{W_L^* + W_R^*}{2} \qquad \text{and} \qquad \delta W = \frac{W_R^* - W_L^*}{2}.
\tag{3.8}
$$

We highlight that this corresponds to rewriting the intermediate states in terms of the unknowns $\widehat{W}$ and δW. Namely, we have $W_L^* = \widehat{W} - \delta W$ and $W_R^* = \widehat{W} + \delta W$. Equipped with this notation, (3.7) immediately gives the following expressions for the components of $\widehat{W}$:

$$
\begin{cases}
\widehat{\rho} = \rho_{\mathrm{HLL}}, \\
\widehat{q} = q_{\mathrm{HLL}} + \dfrac{S^q\Delta x}{2\lambda}, \\
\widehat{E} = E_{\mathrm{HLL}} + \dfrac{S^E\Delta x}{2\lambda}.
\end{cases}
\tag{3.9}
$$

We are thus left with the determination of the three components of δW and of the two source term averages S^q and S^E, i.e., five unknowns to determine in total. However, whatever the expressions of these unknowns, the scheme (3.12) is constructed to satisfy (3.3), and is therefore consistent by definition.

The remainder of Section 3 is devoted to their derivation, ensuring positivity preservation, entropy stability and well-balancedness. However, first, we explain in Section 3.3 how to use the A-RS (3.1) to derive the time update of the numerical scheme, and precisely define in Section 3.4 the properties to be satisfied by the scheme, and thus by the intermediate states.

3.3. **The Godunov-type scheme finite volume scheme.** We start by defining the cell-wise juxtaposition W_Δ of the approximate Riemann solver (3.1), by

$$\forall i \in \mathbb{Z},\, \forall t \in (0, \Delta t],\, \forall x \in (x_i, x_{i+1}),\, W_\Delta(x, t^n + t) = \widetilde{W}\left(\frac{x - x_{i+\frac{1}{2}}}{t}; W_i^n, W_{i+1}^n\right).$$

This definition is illustrated on Figure 2. The time update of the Godunov-type scheme is then given by integrating the juxtaposition W_Δ of Riemann solvers at time $t^{n+1} = t^n + \Delta t$ over each cell C_i, yielding

$$W_i^{n+1} = \frac{1}{\Delta x}\int_{x_{i-\frac{1}{2}}}^{x_{i+\frac{1}{2}}} W_\Delta(x, t^{n+1})dx. \tag{3.10}$$

For stability purposes, we impose the following CFL condition on Δt, see [27]:

$$\Delta t \leq \frac{1}{2}\frac{\Delta x}{\max_i \lambda_{i+\frac{1}{2}}}. \tag{3.11}$$

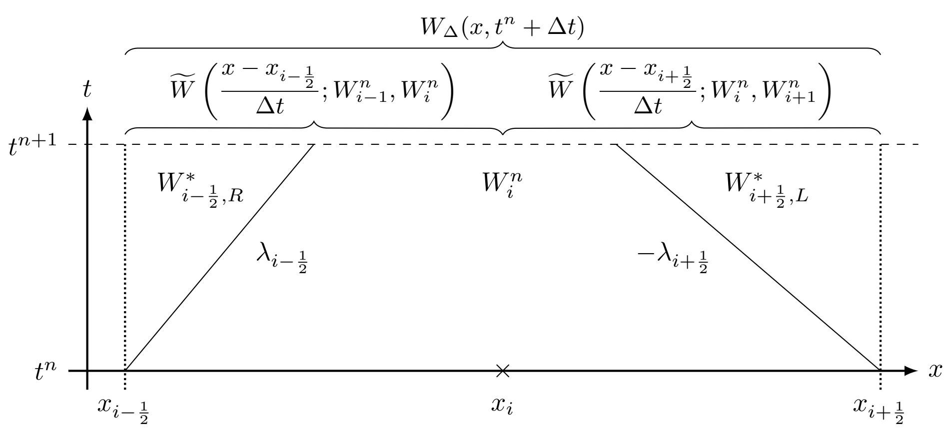

FIGURE 2. Juxtaposition of subsequent A-RSs defining W_Δ using definition (3.14) of the intermediate states $W^*_{i-1/2,R}$ and $W^*_{i+1/2,L}$.

To properly compute the integral in (3.10), we note that W_L^* and W_R^* are given as functions of the left and right states W_L and W_R, as well as of the corresponding left and right gravitational potentials φ_L and φ_R. Since the structure of the A-RS (3.1) comprises a stationary wave with velocity 0, the scheme, see e.g. [33], is given by

(3.12)
$$W_i^{n+1} = W_i^n - \lambda \frac{\Delta t}{\Delta x} \left[W_L^* \left(W_i^n, W_{i+1}^n, \varphi_i, \varphi_{i+1} \right) - W_R^* \left(W_{i-1}^n, W_i^n, \varphi_{i-1}, \varphi_i \right) \right].$$

We emphasize that the scheme (3.12) can also be rewritten in the standard conservation form

$$W_i^{n+1} = W_i^n - \frac{\Delta t}{\Delta x} \left(\mathcal{F}_{i+\frac{1}{2}}^n - \mathcal{F}_{i-\frac{1}{2}}^n \right) + \frac{\Delta t}{2} \left(\mathcal{S}_{i+\frac{1}{2}}^n + \mathcal{S}_{i-\frac{1}{2}}^n \right), \tag{3.13}$$

where $\mathcal{F}_{i+1/2}^n$ is the numerical flux at interface $x_{i+1/2}$, and where $\mathcal{S}_{i+1/2}^n$ is the numerical source term at interface $x_{i+1/2}$. The expressions of $\mathcal{F}_{i+1/2}^n$ and $\mathcal{S}_{i+1/2}^n$ are obtained thanks to straightforward computations presented in e.g. [27]. Setting

$$\begin{aligned} W_{i+1/2,L}^* &= W_L^*(W_{i-1}^n, W_i^n, \varphi_{i-1}, \varphi_i) \quad \text{and} \\ W_{i+1/2,R}^* &= W_R^*(W_{i-1}^n, W_i^n, \varphi_{i-1}, \varphi_i), \end{aligned} \tag{3.14}$$

we obtain

$$\mathcal{F}_{i+\frac{1}{2}}^n = \frac{F(W_i^n) + F(W_{i+1}^n)}{2} - \frac{\lambda_{i+\frac{1}{2}}}{2} \left(W_{i+\frac{1}{2},L}^* - W_i^n \right) + \frac{\lambda_{i+\frac{1}{2}}}{2} \left(W_{i+\frac{1}{2},R}^* - W_{i+1}^n \right).$$

The numerical source term is given by

$$\mathcal{S}_{i+\frac{1}{2}}^n = \begin{pmatrix} 0 \\ (S^q)_{i+\frac{1}{2}}^n \\ (S^E)_{i+\frac{1}{2}}^n \end{pmatrix},$$

where $(S^q)_{i+1/2}^n$ and $(S^E)_{i+1/2}^n$ denote the source term approximations (3.6) evaluated at the interface $x_{i+\frac{1}{2}}$.

By (3.13), or equivalently (3.12), we have defined the time update of the consistent Godunov-type finite volume scheme, up to the definition of the intermediate states W_L^* and W_R^* and source term approximations S^q and S^E. Before giving their derivation, we detail in Section 3.4 the key properties the scheme has to satisfy.

3.4. **Properties to be satisfied by the numerical scheme.** The objective of this section is to state important definitions and give theoretical results. They serve as the backbone for the derivation of the unknowns in the A-RS, to be carried out in Sections 3.5 and 3.6.

3.4.1. *Well-balancedness.* We start with the definition of a well-balanced scheme. We emphasize that we are interested in developing a so-called *fully well-balanced* scheme, which exactly preserves the moving steady solutions described in Section 2.3. As such, the scheme will not preserve all hydrostatic equilibria described in Section 2.2, but only the isentropic ones governed by (2.9), since they are the limit of moving ones when the velocity vanishes.

To properly introduce our definition of well-balancedness, we first need to introduce the notion of interface steady solution (ISS). Indeed, from (2.14), we know that a solution is steady if the discharge q, the total enthalpy H and the specific entropy s are constant. This leads us to the following definition of an ISS.

Definition 3.1 (Interface Steady Solution (ISS))**.** A pair (W_L, W_R) of admissible states is said to be an Interface Steady Solution (ISS) if, and only if,

$$q_L = q_R, \quad H(W_L, \varphi_L) = H(W_R, \varphi_R), \quad \text{and} \quad s(W_L) = s(W_R).$$

Equipped with the definition of the ISS, we can now properly define a well-balanced scheme.

Definition 3.2 (Well-balancedness)**.** Scheme (3.12) is said to be well-balanced if

$$\forall i \in \mathbb{Z},\ (W_i^n, W_{i+1}^n) \text{ is an ISS} \qquad \Longrightarrow \qquad \forall i \in \mathbb{Z},\ W_i^{n+1} = W_i^n.$$

Corollary 3.3. *Let (W_L, W_R) be an ISS. A sufficient condition for well-balancedness is that $W_L^* = W_L$ and $W_R^* = W_R$.*

Proof. Assume that (W_i^n, W_{i+1}^n) and (W_{i-1}^n, W_i^n) are ISSs. We need to show that $W_i^{n+1} = W_i^n$ in order for the scheme to preserve the steady solution. If the intermediate states satisfy $W_L^* = W_L$ and $W_R^* = W_R$, then $W_L^*(W_i^n, W_{i+1}^n, \varphi_i, \varphi_{i+1}) = W_i^n$ and $W_R^*(W_{i-1}^n, W_i^n, \varphi_{i-1}, \varphi_i) = W_i^n$. Plugging these relations into (3.12) immediately yields $W_i^{n+1} = W_i^n$, which concludes the proof. □

According to Corollary 3.3, and recalling the definitions (3.8) of $\widehat{W}$ and δW, the following conditions on these quantities must hold

$$(W_L, W_R) \text{ is an ISS} \qquad \Longrightarrow \qquad \widehat{W} = \frac{W_L + W_R}{2} \quad \text{and} \quad \delta W = \frac{W_R - W_L}{2}. \tag{3.15}$$

Put in other words, (W_L^*, W_R^*) must also be an ISS, i.e.,

$$q_L^* = q_R^*, \qquad H(W_L^*, \varphi_L) = H(W_R^*, \varphi_R) \qquad \text{and} \qquad s(W_L^*) = s(W_R^*). \tag{3.16}$$

For instance, conditions (3.16) lead to a single momentum component for both intermediate states, which we denote by $q^* \coloneqq q_L^* = q_R^*$. Moreover, we define a single intermediate entropy

$$s^* \coloneqq s(W_L^*) = s(W_R^*). \tag{3.17}$$

We will use conditions (3.15) – (3.16) to determine the expressions of δW and S^q, S^E in Section 3.5 and Section 3.6 respectively.

3.4.2. *Entropy stability.* The second important property that we wish to satisfy is entropy stability, defined below.

Definition 3.4 (Entropy stability)**.** The scheme (3.12) is said to be entropy-stable if, for all smooth functions η satisfying (2.7) and for all $i \in \mathbb{Z}$, the states W_i^n and W_i^{n+1} fulfil the discrete entropy inequality

$$\rho_i^{n+1}\eta(s_i^{n+1}) \leq \rho_i^n \eta(s_i^n) - \frac{\Delta t}{\Delta x}\left((\rho\eta(s)u)_{i+1/2}^n - (\rho\eta(s)u)_{i-1/2}^n\right). \tag{3.18}$$

In order to reach this important stability property and since we are considering Godunov-type schemes, we here adopt the well-known integral entropy consistency stated in [27]. As a consequence, the scheme (3.12) will be entropy-preserving by satisfying a discrete entropy inequality (3.18) as soon as the A-RS, given by $\widetilde{W}$ in the form (3.1), verifies

$$\begin{aligned} &\frac{1}{\Delta x}\int_{-\Delta x/2}^{\Delta x/2} \widetilde{(\rho\eta(s))}\left(\frac{x}{\Delta t}, W_L, W_R\right) dx \leq \\ &\qquad \frac{1}{2}\big(\rho_L\eta(s_L) + \rho_R\eta(s_R)\big) - \frac{\Delta t}{\Delta x}\big(\rho_R\eta(s_R)u_R + \rho_L\eta(s_L)u_L\big), \end{aligned} \tag{3.19}$$

where, with abuse of notation, we have defined $s_L = s(W_L)$ and $s_R = s(w_R)$. According to (3.1), we readily show that the integral in (3.19) satisfies

$$\frac{1}{\Delta x}\int_{-\Delta x/2}^{\Delta x/2} \widetilde{(\rho\eta(s))}\left(\frac{x}{\Delta t}, W_L, W_R\right) dx = \left(\frac{1}{2} - \lambda\frac{\Delta t}{\Delta x}\right)\rho_L\eta(s_L) + \lambda\frac{\Delta t}{\Delta x}\rho_L^*\eta(s(W_L^*)) + \lambda\frac{\Delta t}{\Delta x}\rho_R^*\eta(s(W_R^*)) + \left(\frac{1}{2} - \lambda\frac{\Delta t}{\Delta x}\right)\rho_R\eta(s_R),$$

so that, by involving $s(W_L^*) = s(W_R^*) =: s^*$ imposed in (3.17), (3.19) is immediately rewritten as

$$\frac{1}{2}\big(\rho_L^* + \rho_R^*\big)\eta(s^*) \leq \frac{1}{2}\big(\rho_L\eta(s_L) + \rho_R\eta(s_R)\big) - \frac{1}{2\lambda}\big(\rho_R\eta(s_R)u_R + \rho_L\eta(s_L)u_L\big).$$

For the sake of simplicity in the forthcoming notations, in addition to (3.5), we define

$$(\rho s)_{\mathrm{HLL}} = \frac{1}{2}\big(\rho_L s_L + \rho_R s_R\big) - \frac{1}{2\lambda}\big(\rho_R s_R u_R - \rho_L s_L u_L\big), \tag{3.20}$$

$$\big(\rho\eta(s)\big)_{\mathrm{HLL}} = \frac{1}{2}\big(\rho_L\eta(s_L) + \rho_R\eta(s_R)\big) - \frac{1}{2\lambda}\big(\rho_R\eta(s_R)u_R - \rho_L\eta(s_L)u_L\big). \tag{3.21}$$

As a consequence of this notation, and because (3.7) implies that $\rho_L^* + \rho_R^* = 2\rho_{\mathrm{HLL}}$, the integral entropy consistency condition (3.19) to be satisfied by the A-RS now reads

$$\rho_{\mathrm{HLL}}\eta(s^*) \leq \big(\rho\eta(s)\big)_{\mathrm{HLL}}. \tag{3.22}$$

In order to select a suitable definition of s^*, we now state one of our main results.

Theorem 3.5. *Let two given states $W_L \in \Omega$ and $W_R \in \Omega$, and adopt a definition of λ such that $\rho_{HLL} > 0$. Then, for all convex smooth functions η, we have*

$$\eta\left(\frac{(\rho s)_{HLL}}{\rho_{HLL}}\right) \leq \frac{\big(\rho\eta(s)\big)_{HLL}}{\rho_{HLL}}. \tag{3.23}$$

Proof. The establishment of this important result relies on the introduction of a standard HLL scheme for an auxiliary system given by

$$\partial_t\rho + \partial_x(\rho u) = 0, \tag{3.24a}$$

$$\partial_t(\rho u) + \partial_x(\rho u^2 + p) = 0, \tag{3.24b}$$

$$\partial_t(\rho s) + \partial_x(\rho s u), \tag{3.24c}$$

where the pressure law is given by $s = -\log(p/\rho^\gamma)$ as in (2.6). We remark that the weak solutions of the above system satisfy, for all smooth functions g,

$$\partial_t(\rho g(s)) + \partial_x(\rho g(s)u). \tag{3.25}$$

We introduce $U_{\mathcal{R}}(x/t; W_L, W_R)$ the exact Riemann solution of (3.24), and we consider an A-RS, denoted by $\widetilde{U}(x/t; W_L, W_R)$, made of a single intermediate state $(\bar\rho_{\mathrm{HLL}}, \overline{\rho u}_{\mathrm{HLL}}, \overline{\rho s}_{\mathrm{HLL}})$. Once again, by considering the integral consistency condition, here given by

$$\frac{1}{\Delta x}\int_{-\Delta x/2}^{\Delta x/2} \widetilde{U}\left(\frac{x}{\Delta t}; W_L, W_R\right) dx = \frac{1}{\Delta x}\int_{-\Delta x/2}^{\Delta x/2} U_{\mathcal{R}}\left(\frac{x}{\Delta t}; W_L, W_R\right) dx,$$

we get after easy computations

$$\begin{aligned}\bar{\rho}_{\mathrm{HLL}} &= \frac{1}{2}\left(\rho_L + \rho_R\right) - \frac{1}{2\lambda}\left(\rho_R u_R - \rho_L u_L\right),\\ \overline{\rho s}_{\mathrm{HLL}} &= \frac{1}{2}\left(\rho_L s_L + \rho_R s_R\right) - \frac{1}{2\lambda}\left(\rho_R s_R u_R - \rho_L s_L u_L\right).\end{aligned}$$

According to notation (3.5) and (3.20), we remark that

$$\bar{\rho}_{\mathrm{HLL}} = \rho_{\mathrm{HLL}} \qquad \text{and} \qquad \overline{\rho s}_{\mathrm{HLL}} = (\rho s)_{\mathrm{HLL}}. \tag{3.26}$$

Next, we integrate over a space-time slab the equation (3.24c) governing ρs, to get

$$\int_0^{\Delta t}\int_{-\lambda\Delta t}^{\lambda\Delta t}\big(\partial_t(\rho s) + \partial_x(\rho s u)\big)dx\,dt = 0.$$

Computing the integral, we obtain

$$\overline{\rho s}_{\mathrm{HLL}} = \frac{1}{2\lambda\Delta t}\int_{-\lambda\Delta t}^{\lambda\Delta t}(\rho s)_{\mathcal{R}}\left(\frac{x}{\Delta t}; W_L, W_R\right)dx,$$

where $(\rho s)_{\mathcal{R}}$ is the last component of $U_{\mathcal{R}}$. Then, we have

$$\frac{\overline{\rho s}_{\mathrm{HLL}}}{\bar{\rho}_{\mathrm{HLL}}} = \frac{1}{2\lambda\Delta t}\int_{-\lambda\Delta t}^{\lambda\Delta t} s_{\mathcal{R}}\left(\frac{x}{\Delta t}; W_L, W_R\right)\frac{\rho_{\mathcal{R}}\left(\frac{x}{\Delta t}; W_L, W_R\right)dx}{\bar{\rho}_{\mathrm{HLL}}},$$

where we have set $s_{\mathcal{R}} = (\rho s)_{\mathcal{R}}/\rho_{\mathcal{R}}$. Now we notice that the measure

$$\frac{\rho_{\mathcal{R}}\left(\frac{\cdot}{\Delta t}; W_L, W_R\right)dx}{2\lambda\Delta t\bar{\rho}_{\mathrm{HLL}}}$$

is a probability measure over $(-\lambda\Delta t, \lambda\Delta t)$. Hence, for all convex real functions η, Jensen's inequality gives

$$\eta\left(\frac{\overline{\rho s}_{\mathrm{HLL}}}{\bar{\rho}_{\mathrm{HLL}}}\right) \leq \frac{1}{2\lambda\Delta t}\int_{-\lambda\Delta t}^{\lambda\Delta t}\eta\left(s_{\mathcal{R}}\left(\frac{x}{\Delta t}; W_L, W_R\right)\right)\frac{\rho_{\mathcal{R}}\left(\frac{x}{\Delta t}; W_L, W_R\right)dx}{\bar{\rho}_{\mathrm{HLL}}}. \tag{3.27}$$

Next, since $U_{\mathcal{R}}$ defines an exact solution of (3.24), from (3.25) we get, with $g = \eta$,

$$\int_0^{\Delta t}\int_{-\lambda\Delta t}^{\lambda\Delta t}\big(\partial_t(\rho\eta(s)) + \partial_x(\rho\eta(s)u)\big)dx\,dt = 0.$$

We thus easily obtain

$$\begin{aligned}\frac{1}{2\lambda\Delta t}\int_{-\lambda\Delta t}^{\lambda\Delta t}(\rho\eta(s))_{\mathcal{R}}\left(\frac{x}{\Delta t}; W_L, W_R\right)dx = {} & \frac{1}{2}\left(\rho_L\eta(s)_L + \rho_R\eta(s)_R\right)\\ & - \frac{1}{2\lambda}\left(\rho_R\eta(s)_R u_R - \rho_L\eta(s)_L u_L\right).\end{aligned}$$

Arguing notation (3.21), we have

$$\frac{1}{2\lambda\Delta t}\int_{-\lambda\Delta t}^{\lambda\Delta t}(\rho\eta(s))_{\mathcal{R}}\left(\frac{x}{\Delta t}; W_L, W_R\right)dx = (\rho\eta(s))_{\mathrm{HLL}}$$

so that the relation (3.27) now reads

$$\eta\left(\frac{\overline{\rho s}_{\mathrm{HLL}}}{\bar{\rho}_{\mathrm{HLL}}}\right) \leq \frac{(\rho\eta(s))_{\mathrm{HLL}}}{\bar{\rho}_{\mathrm{HLL}}}.$$

Arguing the notation equivalence (3.26), the estimate (3.23) is established, and the proof is thus completed. $\square$

Now, arguing Theorem 3.5, we remark that the required integral entropy consistency condition (3.22) is immediately satisfied as soon as

$$\rho_{\mathrm{HLL}} s^* = (\rho s)_{\mathrm{HLL}}, \tag{3.28}$$

which defines the intermediate entropy s^*.

3.4.3. *Positivity preservation.* After defining entropy stability, we are now able to precisely state the third required property, positivity preservation, and to give additional conditions on the intermediate states. Indeed, since Ω given by (2.4) is a non-convex set, entropy stability is crucial for a part of the positivity proof.

Definition 3.6 (Positivity preservation)**.** Let $W_i^n \in \Omega$ for all $i \in \mathbb{Z}$ and $n \geq 0$. The scheme (3.12) is said to be positivity-preserving if, for all $i \in \mathbb{Z}$, $W_i^{n+1} \in \Omega$, where Ω is the set of admissible states defined in (2.4).

First, we recall that $\rho_{\mathrm{HLL}} > 0$ under suitable conditions on λ. Indeed, we have

$$\rho_{\mathrm{HLL}} = \frac{\rho_L}{2\lambda}(\lambda + u_L) + \frac{\rho_R}{2\lambda}(\lambda - u_R).$$

As a consequence, with $\rho_L > 0$ and $\rho_R > 0$, the required positiveness of ρ_{HLL} is satisfied as soon as $\lambda > \max(|u_L|, |u_R|)$, which is the case here since λ is given by (3.2). Next, a way to ensure positivity preservation on ρ_i^{n+1} is to impose that $\rho_L^* > 0$ and $\rho_R^* > 0$. Indeed, in this case, all densities in the Riemann fan are positive, which implies the positivity of the density at time t^{n+1}. Moreover, recall that $\rho_L^* = \rho_{\mathrm{HLL}} - \delta\rho$ and $\rho_R^* = \rho_{\mathrm{HLL}} + \delta\rho$. Therefore, a sufficient condition for the positivity of density is

$$|\delta\rho| < \rho_{\mathrm{HLL}}. \tag{3.29}$$

Now, with $\rho_L^* > 0$ and $\rho_R^* > 0$, under assumption (3.29), we may also exhibit a natural condition to get a positive updated pressure $p(W_i^{n+1})$. In fact, we argue the discrete entropy inequality to address this issue.

Lemma 3.7 (Positivity of the pressure)**.** *Let two given states $W_L \in \Omega$ and $W_R \in \Omega$, and adopt a definition of λ such that $\rho_{HLL} > 0$. Moreover, let $\rho_L^* > 0$ and $\rho_R^* > 0$, and consider s^* given by (3.28). Then, for all $i \in \mathbb{Z}$, $p^{i+1} > 0$.*

Proof. Since $W \mapsto \rho\eta(s)$ is convex, by applying Jensen's inequality to the integral form of W_i^{n+1} given by (3.10), we obtain

$$\rho_i^{n+1}\eta(s(W_i^{n+1})) \leq \frac{1}{\Delta x}\int_{x_{i-\frac{1}{2}}}^{x_{i+\frac{1}{2}}} \rho_\Delta(x, t^{n+1})\eta(s_\Delta(x, t^{n+1}))dx,$$

where we have set $s_\Delta = s(W_\Delta)$. Using the definition (2.6) of s, we have

$$\eta\left(-\log\left(\frac{p(W_i^{n+1})}{\rho_i^{n+1}}\right)\right) \leq \int_{x_{i-\frac{1}{2}}}^{x_{i+\frac{1}{2}}} \eta\left(-\log\left(\frac{p(W_\Delta(x, t^{n+1}))}{(\rho_\Delta(x, t^{n+1}))^\gamma}\right)\right) \frac{\rho_\Delta(x, t^{n+1})dx}{\Delta x \rho_i^{n+1}}. \tag{3.30}$$

Moreover, we remark that, since $\rho_i^{n+1} > 0$, the measure defined by

$$\frac{\rho_\Delta(\cdot, t^{n+1})dx}{\Delta x \rho_i^{n+1}} = \frac{\rho_\Delta(\cdot, t^{n+1})dx}{\int_{x_{i-\frac{1}{2}}}^{x_{i+\frac{1}{2}}} \rho_\Delta(x, t^{n+1})dx}$$

is a probability measure over $(x_{i-1/2}, x_{i+1/2})$. Now, let us introduce the function

$$\begin{aligned}\Xi : (0,+\infty) &\to \mathbb{R}\\ z &\mapsto \eta(-\log(z)).\end{aligned}$$

Equipped with the properties (2.7) of η, it is easy to show that Ξ is a monotonically decreasing and convex function. Therefore, it is invertible, and its inverse Ξ^{-1} is monotonically decreasing and concave. Applying Ξ^{-1} to (3.30) yields

$$\frac{p(W_i^{n+1})}{\rho_i^{n+1}} \geq \Xi^{-1}\left(\int_{x_{i-\frac{1}{2}}}^{x_{i+\frac{1}{2}}} \Xi\left(\frac{p(W_\Delta(x,t^{n+1}))}{(\rho_\Delta(x,t^{n+1}))^\gamma}\right)\frac{\rho_\Delta(x,t^{n+1})dx}{\Delta x \rho_i^{n+1}}\right).$$

Since Ξ^{-1} is a concave function, applying Jensen's inequality to the right-hand side of the above inequality, we obtain

$$\frac{p(W_i^{n+1})}{(\rho_i^{n+1})^\gamma} \geq \int_{x_{i-\frac{1}{2}}}^{x_{i+\frac{1}{2}}} \frac{p(W_\Delta(x,t^{n+1}))}{(\rho_\Delta(x,t^{n+1}))^\gamma}\frac{\rho_\Delta(x,t^{n+1})}{\Delta x \rho_i^{n+1}}\,dx.$$

Since $W_\Delta(x,t^{n+1})$ is a juxtaposition of A-RSs defined by (3.1), because of the positiveness of ρ_i^{n+1} and $\rho_\Delta(x,t^{n+1})$ given by both $\rho_L^* > 0$ and $\rho_R^* > 0$, it results that $p(W_i^{n+1}) > 0$ as soon as

$$p(W_L^*) > 0 \qquad \text{and} \qquad p(W_R^*) > 0.$$

Moreover, according to the definition (2.6) of s, the pressures of the intermediate states satisfy $p(W_L^*) = (\rho_L^*)^\gamma \exp(-s^*)$ and $p(W_R^*) = (\rho_R^*)^\gamma \exp(-s^*)$. Thus, the above positivity condition always holds, and $p(W_i^{n+1})$ is therefore positive. □

Equipped with these definitions and conditions (3.15) – (3.16) – (3.28) – (3.29), we now have all the ingredients we need to determine δW in Section 3.5, and S^q, S^E in Section 3.6.

3.5. **Determination of δW.** The goal of this section is to use the definitions from Section 3.4 to derive an expression of the three components of δW, with respect to the left and right states W_L and W_R and the corresponding left and right gravitational potentials φ_L and φ_R. We seek expressions of $\delta\rho$, δq and δE, such that $\delta W = [W]/2$ as soon as (W_L, W_R) is an ISS, where we have denoted by $[X] \coloneqq X_R - X_L$ the jump of some quantity X. Moreover, for stability purposes, we wish to recover the HLL solver in the absence of a gravitational source term. Therefore, we also impose that, if $\varphi_L = \varphi_R$, then δW must vanish.

We start with the momentum component δq. Note that, according to (3.16), we set $q_L^* = q_R^*$. Therefore, $\delta q = 0$ is a suitable choice.

Now, we turn to the density component $\delta\rho$. Recall that, if (W_L, W_R) is an ISS, then $H(W_L, \varphi_L) = H(W_R, \varphi_R)$, that is to say

$$\frac{E_L + p_L}{\rho_L} + \varphi_L = \frac{E_R + p_R}{\rho_R} + \varphi_R. \tag{3.31}$$

Defining the enthalpy

$$h = \frac{E + p}{\rho}, \tag{3.32}$$

and setting $h_L = h(W_L)$ and $h_R = h(W_R)$, (3.31) rewrites as

$$[h] = -[\varphi]. \tag{3.33}$$

In other words, if $[h] \neq 0$, then

$$y \coloneqq 1 + \frac{[\varphi]}{[h]} = 0. \tag{3.34}$$

The function $y \mapsto \delta\rho(y)$ must then fulfil the following properties:

(i) $$\delta\rho(0) = [\rho]/2,$$

(ii) $$\delta\rho(1) = 0,$$

(iii) $$|\delta\rho| < \rho_{\mathrm{HLL}},$$

(iv) $$\lim_{y\to\pm\infty} \delta\rho(y) = 0.$$

Property (i) corresponds to the ISS case, and ensures that $\delta\rho$ satisfies (3.15). Property (ii) corresponds to the no-gravity case, since $y = 1$ as soon as $[\varphi] = 0$. In this case, we wish $\delta\rho$ to vanish, so that $\rho_L^* = \rho_R^* = \rho_{\mathrm{HLL}}$. Property (iii) is the required condition (3.29) for positivity preservation. Property (iv) ensures that $\delta\rho$ is well-defined and goes to 0 when $[h]$ vanishes. To determine the final expression of $\delta\rho$ satisfying properties (i) – (iv), we first introduce a relevant function ψ.

Lemma 3.8. *Let ψ be a smooth function given by*

$$\psi(y) = \cos\left(\frac{\pi}{2}y\right)\exp\left(-2y^2\right). \tag{3.35}$$

Then ψ satisfies the following properties:

(ψ-i) $$\psi(0) = 1,$$

(ψ-ii) $$\psi(1) = 0,$$

(ψ-iii) $$|\psi| \leq 1,$$

(ψ-iv) $$\lim_{y\to\pm\infty} \psi(y) = 0,$$

(ψ-v) $$\psi(1+y) = \mathcal{O}(y) \qquad \textit{as} \quad y \to 0.$$

Proof. Properties (ψ-i) and (ψ-ii) are straightforward to verify by inspection. For completeness, we provide in Figure 3 a graphical representation of ψ. For property (ψ-iii), we note that for all $y \in \mathbb{R}$,

$$|\psi(y)| = \left|\cos\left(\frac{\pi}{2}y\right)\exp\left(-2y^2\right)\right| \leq \exp(-2y^2) \leq 1.$$

Property (ψ-iv) holds since cos is a bounded function and $y \mapsto e^{-2y^2}$ goes to 0 as y goes to $\pm\infty$. Finally, to prove property (ψ-v), we compute $\psi(1+y)$ for $y \in \mathbb{R}$. We obtain

$$\psi(1+y) = \cos\left(\frac{\pi}{2} + \frac{\pi}{2}y\right)\exp\left(-2(1+y)^2\right) = -\sin\left(\frac{\pi}{2}y\right)\exp\left(-2(1+y)^2\right).$$

Therefore,

$$\psi(1+y) \sim -\frac{\pi}{2}e^{-2}y \qquad \text{as} \quad y \to 0,$$

which proves (ψ-v) and concludes the proof. □

We now have all the ingredients we need to construct $\delta\rho$ as a function of y. Note that multiple expressions of such a function $y \mapsto \delta\rho(y)$ are possible. We give the chosen smooth expression below, and prove that it satisfies the above properties.

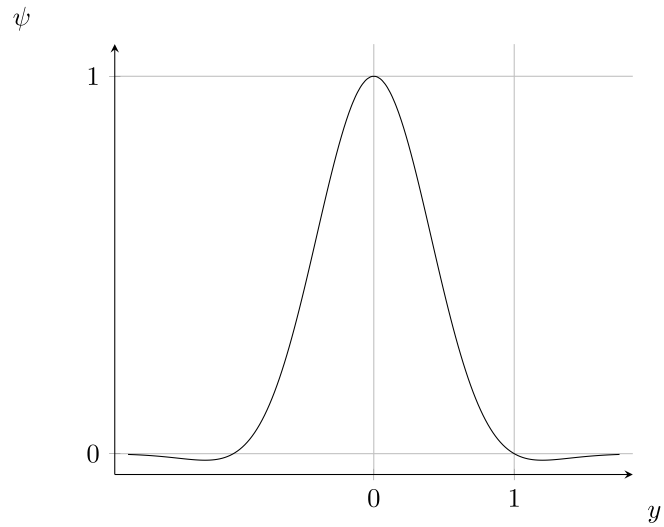

FIGURE 3. Graph of the function ψ defined in Lemma 3.8. We observe that ψ indeed satisfies properties (ψ-i) – (ψ-iv).

Lemma 3.9. *Let $y \mapsto \delta\rho(y)$ be a smooth function given by*

$$\delta\rho(y) = \frac{[\rho]}{2}\psi(y),$$

where y is defined by (3.34) and ψ is given by (3.35). Then, conditions (i) – (iv) are satisfied by $\delta\rho(y)$.

Proof. First, we note that the properties (ψ-i), (ψ-ii) and (ψ-iv) directly map to properties (i), (ii) and (iv). Second, to prove property (iii), we need to show that $|\delta\rho| < \rho_{\mathrm{HLL}}$. To that end, we analyze the extrema of the function $\delta\rho(y)$. According to property (ψ-iii) of ψ, the global extremum of $\delta\rho(y)$ is $[\rho]/2$, reached for $y = 0$. Therefore, since $\rho_L > 0$ and $\rho_R > 0$, we immediately obtain

$$|\delta\rho| \leq \frac{|\rho_R - \rho_L|}{2} \leq \frac{\rho_L + \rho_R}{2}.$$

Hence, according to the expression (3.5) of ρ_{HLL}, there exists a large enough λ such that $|\delta\rho| < \rho_{\mathrm{HLL}}$, and property (iii) is satisfied. The proof is thus concluded. $\square$

Finally, we turn to the energy component δE. Analogously to the derivation of δq and $\delta\rho$, we use the last remaining ISS condition on s to determine δE. Namely, we wish to impose that $s(W_L^*) = s(W_R^*)$ as soon as (W_L, W_R) is an ISS, as prescribed in (3.16). Note that this implies, using the definition (2.6) of s, that

$$-\log\left(\frac{p(W_L^*)}{(\rho_L^*)^\gamma}\right) = -\log\left(\frac{p(W_R^*)}{(\rho_R^*)^\gamma}\right), \quad \text{thus,} \quad \frac{p(W_L^*)}{(\rho_L^*)^\gamma} = \frac{p(W_R^*)}{(\rho_R^*)^\gamma}.$$

Therefore, using the expression (2.2) of the pressure law, we obtain

$$\frac{1}{(\rho_L^*)^\gamma}\left(E_L^* - \frac{\widetilde{q}^2}{2\rho_L^*}\right) = \frac{1}{(\rho_R^*)^\gamma}\left(E_R^* - \frac{\widetilde{q}^2}{2\rho_R^*}\right), \tag{3.36}$$

where $\widetilde{q^2}$ denotes an average of q^2 which will be determined later on. Arguing $E_L^* = \widehat{E} - \delta E$ and $E_R^* = \widehat{E} + \delta E$ leads to the following expression of δE

$$\delta E = \frac{1}{(\rho_L^*)^\gamma + (\rho_R^*)^\gamma} \left((\rho_R^*)^\gamma \left(\widehat{E} - \frac{\widetilde{q^2}}{2\rho_L^*} \right) - (\rho_L^*)^\gamma \left(\widehat{E} - \frac{\widetilde{q^2}}{2\rho_R^*} \right) \right). \tag{3.37}$$

Note that this expression of δE satisfies both properties required for well-balancedness, independently of the expression of $\widetilde{q^2}$. Hence, $\widetilde{q^2}$ is a degree of freedom in the numerical scheme. It turns out that one can determine $\widetilde{q^2}$ such that the scheme is entropy-satisfying, by leveraging condition (3.28) on the intermediate entropy s^*. Indeed, recall that we have defined $s^* = s(W_L^*) = s(W_R^*)$, and that s^* is defined by $s^* = (\rho s)_{\mathrm{HLL}}/\rho_{\mathrm{HLL}}$. By definition of a constant-entropy intermediate state, we obtain

$$-\log\left(\frac{p(W_L^*)}{(\rho_L^*)^\gamma} \right) = s^* = \frac{(\rho s)_{\mathrm{HLL}}}{\rho_{\mathrm{HLL}}}.$$

Therefore, taking the exponential of minus both sides leads to

$$\frac{1}{(\rho_L^*)^\gamma} \left(\widehat{E} - \delta E - \frac{\widetilde{q^2}}{2\rho_L^*} \right) = \frac{1}{\gamma - 1} \exp\left(-\frac{(\rho s)_{\mathrm{HLL}}}{\rho_{\mathrm{HLL}}} \right).$$

Substituting δE by (3.37) in this relation leads, after straightforward computations, to

$$\widetilde{q^2} = \frac{2\rho_L^* \rho_R^*}{\rho_L^* + \rho_R^*} \left(2\widehat{E} - \exp\left(-\frac{(\rho s)_{\mathrm{HLL}}}{\rho_{\mathrm{HLL}}} \right) \frac{(\rho_L^*)^\gamma + (\rho_R^*)^\gamma}{\gamma - 1} \right).$$

Note that this expression is indeed consistent with a squared momentum, since the expression in brackets is consistent with a kinetic energy.

Remark 3.10 (Dependence on the EOS). Note that the definition of the EOS enters the derivation of the states δW for the first time in equation (3.36) to obtain δE from the entropy ISS (3.16) to reformulate $s(W_L^*) = s(W_R^*)$. This indicates that a change of EOS merely implies the adaptation of δE and $\widetilde{q^2}$.

3.6. **Determination of S^q and S^E.** Equipped with the expression of δW, we now turn to the determination of the last two unknowns, S^q and S^E. To that end, we leverage the expressions (3.9) of $\widehat{W}$, and recall that, if (W_L, W_R) is an ISS, then $\widehat{W} = \overline{W}$, where we have defined $\overline{X} \coloneqq (X_L + X_R)/2$ the arithmetic mean of two quantities X_L and X_R. Therefore, plugging the expression of W_{HLL} in (3.9), we obtain that, if (W_L, W_R) is an ISS, then S^q and S^E must satisfy

$$S^q \Delta x = \left(\frac{q_R^2}{\rho_R} + p_R \right) - \left(\frac{q_L^2}{\rho_L} + p_L \right), \tag{3.38a}$$

$$S^E \Delta x = \left(\frac{q_R}{\rho_R}(E_R + p_R) \right) - \left(\frac{q_L}{\rho_L}(E_L + p_L) \right). \tag{3.38b}$$

Moreover, recall that S^q and S^E should be consistent approximations of the source term averages. Therefore, the goal of this section is to find such consistent averages satisfying (3.38).

Remark 3.11. Since φ is assumed to be a smooth function, for each interface, the following identities hold:

$$\varphi_R = \varphi_L + \mathcal{O}(\Delta x), \quad \text{i.e.,} \quad [\varphi] = \mathcal{O}(\Delta x).$$

We start with the energy source term S^E. Its expression and related properties are given in the following lemma.

Lemma 3.12. *Let two given states $W_L \in \Omega$ and $W_R \in \Omega$. Further, let*

$$S^E = -\frac{q_L + q_R}{2}\,\frac{\varphi_R - \varphi_L}{\Delta x}. \tag{3.39}$$

Then S^E is consistent with $-q\partial_x\varphi$ and satisfies the well-balanced condition (3.38b).

Proof. To prove consistency with the continuous source term, we take $q_L = q(x)$ and $q_R = q(x + \Delta x)$, with $\varphi_L = \varphi(x)$ and $\varphi_R = \varphi(x + \Delta x)$. Arguing Remark 3.11, a simple Taylor expansion of S^E then shows that $S^E = -q\partial_x\varphi + \mathcal{O}(\Delta x)$, which proves the consistency of S^E.

For the well-balancedness, recall that the enthalpy is given in (3.32) and satisfies $E + p = \rho h$. So, if (W_L, W_R) is an ISS with $q_L = q_R = \bar{q}$, then $S^E\Delta x$ must satisfy $S^E\Delta x = \bar{q}(h_R - h_L)$ after (3.38b). However, from (3.33) we have that $[h] = -[\varphi]$ if (W_L, W_R) is an ISS. Therefore, S^E given by (3.39) satisfies (3.38b) by construction, which concludes the proof. □

Next, we consider the momentum source term S^q. Its expression and derivation are more involved; they are summarized in the following lemma.

Lemma 3.13. *Let two given states $W_L \in \Omega$ and $W_R \in \Omega$. Further, let*

$$S^q = -\frac{2\rho_L\rho_R}{\rho_L + \rho_R}\,\frac{\varphi_R - \varphi_L}{\Delta x} + \frac{\varepsilon}{\Delta x}\,\psi\left(1 + \left(\frac{\varphi_R - \varphi_L}{h_R - h_L}\right)^3\right), \tag{3.40}$$

where ψ is given by (3.35) and ε is given by

$$\varepsilon = \overline{e^{-s}}\left((\rho_R^\gamma - \rho_L^\gamma) - \frac{2\rho_L\rho_R}{\rho_L + \rho_R}\,\frac{\gamma}{\gamma - 1}\,\left(\rho_R^{\gamma-1} - \rho_L^{\gamma-1}\right)\right), \tag{3.41}$$

with $\overline{e^{-s}} = (e^{-s_L} + e^{-s_R})/2$. Then S^q is consistent with $-\rho\partial_x\varphi$ and satisfies the well-balanced condition (3.38a).

Proof. We first prove that S^q is consistent with the continuous source term. In this context, we emphasize that (W_L, W_R) is not necessarily an ISS, but rather a general pair of states. Performing a Taylor expansion of the first term of S^q, and recalling Remark 3.11, we immediately see that

$$-\frac{2\rho_L\rho_R}{\rho_L + \rho_R}\,\frac{\varphi_R - \varphi_L}{\Delta x} \underset{\Delta x \to 0}{=} -\rho\partial_x\varphi + \mathcal{O}(\Delta x).$$

For the second term of S^q, we distinguish two cases: either the solution is smooth and $W_R = W_L + \mathcal{O}(\Delta x)$, or the solution is not smooth (e.g. in a shock wave) and $W_R = W_L + \mathcal{O}(1)$. It turns out that the multiplication by ψ in (3.40) is crucial to overcome a consistency defect in the non-smooth case. In the first case, performing a Taylor expansion of ε given by (3.41) and noting that $[\varphi]/[h] = \mathcal{O}(1)$ since both $[\varphi]$ and $[h]$ are $\mathcal{O}(\Delta x)$, we obtain that

$$W_R = W_L + \mathcal{O}(\Delta x) \implies \varepsilon = \mathcal{O}(\Delta x^3) \quad \text{and} \quad \psi\left(1 + \frac{[\varphi]^3}{[h]^3}\right) = \mathcal{O}(1).$$

In the second case, arguing property (ψ-v) of ψ and remarking that $[\varphi] = \mathcal{O}(\Delta x)$ and $[h] = \mathcal{O}(1)$, we get

$$W_R = W_L + \mathcal{O}(1) \implies \varepsilon = \mathcal{O}(1) \quad \text{and} \quad \psi\left(1 + \frac{[\varphi]^3}{[h]^3}\right) = \mathcal{O}\left(\frac{[\varphi]^3}{[h]^3}\right) = \mathcal{O}(\Delta x^3).$$

As a consequence, in both cases, the second term of S^q is consistent with 0, with an error of $\mathcal{O}(\Delta x^2)$. Therefore, we have obtained that S^q was indeed consistent with the continuous source term, i.e., that $S^q = -\rho\partial_x\varphi + \mathcal{O}(\Delta x)$.

We now turn to the well-balanced property; we have to prove that S^q, given by (3.40), satisfies (3.38a) as soon as (W_L, W_R) is an ISS. In this case, we recall that $[\varphi] = -[h]$. Therefore, arguing property (ψ-i) of ψ, we obtain $\psi(1+([\varphi]/[h])^3) = 1$. Hence, we have to prove that

$$-\frac{2\rho_L\rho_R}{\rho_L+\rho_R}(\varphi_R-\varphi_L)+\varepsilon = \left(\frac{q_R^2}{\rho_R}+p_R\right)-\left(\frac{q_L^2}{\rho_L}+p_L\right)$$

as soon as (W_L, W_R) is an ISS and for ε given by (3.41). To that end, we first tackle ε. Note that, since we are considering an ISS, we have $s_L = s_R$. Therefore,

$$\overline{e^{-s}} = \frac{1}{2}\left(e^{-s_L}+e^{-s_R}\right) = \frac{1}{2}\left(\frac{p_L}{\rho_L^\gamma}+\frac{p_R}{\rho_R^\gamma}\right) = \frac{p_L}{\rho_L^\gamma} = \frac{p_R}{\rho_R^\gamma}.$$

Using these identities to distribute $\overline{e^{-s}}$, ε rewrites

$$\varepsilon = (p_R-p_L) - \frac{2\rho_L\rho_R}{\rho_L+\rho_R}\frac{\gamma}{\gamma-1}\left(\frac{p_R}{\rho_R}-\frac{p_L}{\rho_L}\right),$$

and, from the expression (3.40) of S^q, we obtain

$$S^q\Delta x = (p_R-p_L) - \frac{2\rho_L\rho_R}{\rho_L+\rho_R}\left((\varphi_R-\varphi_L)+\frac{\gamma}{\gamma-1}\left(\frac{p_R}{\rho_R}-\frac{p_L}{\rho_L}\right)\right). \tag{3.42}$$

Now, using the steady relation $[\varphi] = -[h]$ together with the definition (2.13) of h, we get

$$\varphi_R-\varphi_L = -\left(\frac{E_R+p_R}{\rho_R}-\frac{E_L+p_L}{\rho_L}\right) = -\frac{\gamma}{\gamma-1}\left(\frac{p_R}{\rho_R}-\frac{p_L}{\rho_L}\right)-\left(\frac{1}{2}\frac{q_R^2}{\rho_R^2}-\frac{1}{2}\frac{q_L^2}{\rho_L^2}\right).$$

Plugging this relation into (3.42), the term in brackets reduces to

$$(\varphi_R-\varphi_L)+\frac{\gamma}{\gamma-1}\left(\frac{p_R}{\rho_R}-\frac{p_L}{\rho_L}\right) = -\left(\frac{1}{2}\frac{q_R^2}{\rho_R^2}-\frac{1}{2}\frac{q_L^2}{\rho_L^2}\right).$$

Now, recall that one of the ISS relations is $q_L = q_R = \bar{q}$. Consequently, we obtain

$$\frac{2\rho_L\rho_R}{\rho_L+\rho_R}\left(\frac{1}{2}\frac{q_R^2}{\rho_R}-\frac{1}{2}\frac{q_L^2}{\rho_L}\right) = \bar{q}^2\frac{2\rho_L\rho_R}{\rho_L+\rho_R}\left(\frac{1}{\rho_R^2}-\frac{1}{\rho_L^2}\right) = \bar{q}^2\left(\frac{1}{\rho_R}-\frac{1}{\rho_L}\right) = \frac{q_R^2}{\rho_R}-\frac{q_L^2}{\rho_L}.$$

Substituting into (3.42) leads to

$$S^q\Delta x = (p_R-p_L)+\left(\frac{q_R^2}{\rho_R}-\frac{q_L^2}{\rho_L}\right),$$

which is nothing but the well-balancedness condition (3.38b). The proof is thus concluded. □

3.7. **Summary of the numerical scheme and main properties.** The goal of this section is to summarize the approximate Riemann solver and state the main properties of the scheme deriving from this A-RS. The A-RS (3.1) is given by

$$\widetilde{W}\left(\frac{x}{t}; W_L, W_R\right) = \begin{cases} W_L & \text{if } x < -\lambda t, \\ W_L^* = \widehat{W} - \delta W & \text{if } -\lambda t < x < 0, \\ W_R^* = \widehat{W} + \delta W & \text{if } 0 < x < \lambda t, \\ W_R & \text{if } x > \lambda t. \end{cases} \tag{3.43}$$

This A-RS is based on the HLL solver, whose intermediate state is given by (3.5), with the wave speed λ given by (3.2). Recall also the pressure law (2.2) defining p, the expression (2.6) of the entropy s, and the expression (2.13) of the enthalpy h. Equipped with these definitions, (3.9) gives the following expression of $\widehat{W}$:

$$\begin{cases} \widehat{\rho} = \rho_{\mathrm{HLL}}, \\ \widehat{q} = q_{\mathrm{HLL}} + \dfrac{S^q \Delta x}{2\lambda}, \\ \widehat{E} = E_{\mathrm{HLL}} + \dfrac{S^E \Delta x}{2\lambda}, \end{cases} \tag{3.44}$$

where the approximate source terms S^q and S^E have been derived in Section 3.6 and are given by

$$\begin{aligned} S^E &= -\frac{q_L + q_R}{2} \, \frac{\varphi_R - \varphi_L}{\Delta x}, \\ S^q &= -\frac{2\rho_L \rho_R}{\rho_L + \rho_R} \, \frac{\varphi_R - \varphi_L}{\Delta x} + \frac{\varepsilon}{\Delta x} \, \psi\left(1 + \left(\frac{\varphi_R - \varphi_L}{h_R - h_L}\right)^3\right), \end{aligned} \tag{3.45}$$

where $\psi(y) = \cos(\frac{\pi}{2} y) e^{-2y^2}$, and where ε satisfies

$$\varepsilon = \frac{1}{2}\left(e^{-s_L} + e^{-s_R}\right)\left((\rho_R^\gamma - \rho_L^\gamma) - \frac{2\rho_L\rho_R}{\rho_L + \rho_R} \, \frac{\gamma}{\gamma - 1} \left(\rho_R^{\gamma-1} - \rho_L^{\gamma-1}\right)\right).$$

The components of δW have been derived in Section 3.5, and we have set

$$\begin{cases} \delta\rho = \dfrac{\rho_R - \rho_L}{2} \, \psi\left(1 + \dfrac{\varphi_R - \varphi_L}{h_R - h_L}\right), \\ \delta\rho = 0, \\ \delta E = \dfrac{1}{(\rho_L^*)^\gamma + (\rho_R^*)^\gamma}\left((\rho_R^*)^\gamma\left(\widehat{E} - \dfrac{\widetilde{q^2}}{2\rho_L^*}\right) - (\rho_L^*)^\gamma\left(\widehat{E} - \dfrac{\widetilde{q^2}}{2\rho_R^*}\right)\right), \end{cases} \tag{3.46}$$

where $\widetilde{q^2}$ satisfies

$$\widetilde{q^2} = \frac{2\rho_L^*\rho_R^*}{\rho_L^* + \rho_R^*}\left(2\widehat{E} - \exp\left(-\frac{(\rho s)_{\mathrm{HLL}}}{\rho_{\mathrm{HLL}}}\right) \frac{(\rho_L^*)^\gamma + (\rho_R^*)^\gamma}{\gamma - 1}\right).$$

Equipped with these expressions, we are ready to state our main result, summarizing all properties of the resulting scheme.

Theorem 3.14. *Let the time step Δt be given by (3.11) and assume that the initial data satisfies $W_i^0 \in \Omega$ for all $i \in \mathbb{Z}$. Then, the numerical scheme (3.12) with the approximate Riemann solver (3.43), where $\widehat{W}$ is given by (3.44) and δW is given by (3.46), satisfies the following properties:*

(1) consistency with the Euler system (2.1);

(2) positivity preservation: for all $n \geq 0$,

$$\forall i \in \mathbb{Z},\ W_i^n \in \Omega \quad \Longrightarrow \quad \forall i \in \mathbb{Z},\ W_i^{n+1} \in \Omega;$$

(3) entropy stability: for all smooth functions η satisfying (2.7), for all $i \in \mathbb{Z}$, for all $n \geq 0$,

$$\rho_i^{n+1} \eta(s_i^{n+1}) \leq \rho_i^n \eta(s_i^n) - \frac{\Delta t}{\Delta x}\left((\rho\eta(s)u)_{i+1/2}^n - (\rho\eta(s)u)_{i-1/2}^n\right);$$

(4) *well-balancedness:*

$$\forall i \in \mathbb{Z},\ (W_i^n, W_{i+1}^n) \text{ is an ISS} \quad \Longrightarrow \quad \forall i \in \mathbb{Z},\ W_i^{n+1} = W_i^n.$$

Proof. We prove the four properties in order, using the results derived in the previous sections.

(1) According to [27], the scheme is consistent as soon as the A-RS satisfies the integral consistency relation (3.3), which holds by construction, as detailed in Section 3.2. Thus, the A-RS is consistent, and therefore the numerical scheme (3.12) is also consistent.
(2) We have to prove the positivity of the density and the pressure. A sufficient condition for the positivity of the intermediate density is given by (3.29). It is satisfied thanks to Lemma 3.9, which yields $\rho_L^* > 0$ and $\rho_R^* > 0$ in the A-RS, and thus $\rho_i^{n+1} > 0$ in the numerical scheme. As a consequence, Lemma 3.7 can be applied, yielding the positivity of the pressure $p_i^{n+1} > 0$.
(3) After [27], the entropy stability holds as soon as (3.19) is satisfied. However, following Theorem 3.5, this relation is verified if the intermediate entropy of the A-RS is given by (3.28), which is the case for the A-RS (3.43). This proves that the scheme is entropy-stable.
(4) A sufficient condition for well-balancedness is given in Corollary 3.3, from which follow the sufficient conditions (3.15) to be satisfied by $\widehat{W}$ and δW in the intermediate states of the A-RS. As shown in Sections 3.5 and 3.6, these conditions are satisfied by construction, and consequently the numerical scheme is fully well-balanced.

Thus, all four properties have been proven, which concludes the proof. $\square$

4. A well-balanced higher order extension

See [4].

$$\theta_{i+\frac{1}{2}}^{n+1} = \frac{\varepsilon_{i+\frac{1}{2}}^n}{\varepsilon_{i+\frac{1}{2}}^n + \left(\dfrac{\Delta t}{C_{i+\frac{1}{2}}^n}\right)^{d+1}}, \quad \text{where } \ \varepsilon_{i+\frac{1}{2}}^n = \left\| \begin{pmatrix} q_{i+1}^n - q_i^n \\ H(W_{i+1}^n, \varphi_{i+1}^n) - H(W_i^n, \varphi_{i+1}^n) \\ s(W_{i+1}^n) - s(W_i^n) \end{pmatrix} \right\|.$$

$$C_{i+\frac{1}{2}}^n = C_\theta \, \frac{1}{2} \left(\frac{\|W_{i+1}^n - W_{i+1}^{n-1}\|}{2} + \frac{\|W_i^n - W_i^{n-1}\|}{2} \right) \qquad \text{if } n \geq 1.$$

TODO: mention that we reconstruct in primitive variables

5. Numerical results

In this section, we perform numerical test cases to validate the theoretical properties of the first, second and third order well-balanced scheme, using the polynomials $\mathbb{P}_0, \mathbb{P}_1^{\mathrm{WB}}$ and $\mathbb{P}_2^{\mathrm{WB}}$ respectively for the reconstruction. For all test cases, we consider the isentropic EOS with $\gamma = 1.4$. Throughout these tests, we will use the gravitational potentials $\varphi_1(x) = (x - 0.5)^2/2$ and $\varphi_2(x) = \sin(x)$. Unless otherwise mentioned, the parameter Λ in (3.2) is set to 1.

TODO: talk about the C_θ from the HO schemes, always 1 unless other stated

5.1. **Accuracy of the numerical schemes.** To verify the experimental order of convergence (EOC) of the numerical schemes, we study an exact solution for the Euler equations with gravity (2.1) taken from [31], which is a variation of the test introduced in [40]. The analytical solution is given by

$$
\begin{aligned}
\rho(x,t) &= 1 + \frac{1}{5}\sin(k\pi(x-u_0t)),\\
u(x,t) &= u_0,\\
p(x,t) &= \frac{9}{2} - (x-u_0t) + \frac{1}{k\pi}\cos(k\pi(x-u_0t)),
\end{aligned} \tag{5.1}
$$

where u_0 is a constant velocity, taken as $u_0 = 1$ in the experiment. We take $k = 5$, which yields a highly oscillatory solution. This test case is designed for a linear potential $\varphi(x) = x$. The simulation is carried out on the computational domain $\Omega = [0,2]$ up to a final time of $t_f = 0.1$, on seven grids with $N = 16 \cdot 2^j$ cells, where $j \in \{0,\dots,6\}$. We prescribe exact boundary conditions. In Figure 4, the L^2 errors are depicted with respect to the number of cells. We recover the expected order of convergence for all schemes. Namely, we observe that the high-order well-balanced correction does not negatively affect the convergence rate of the scheme.

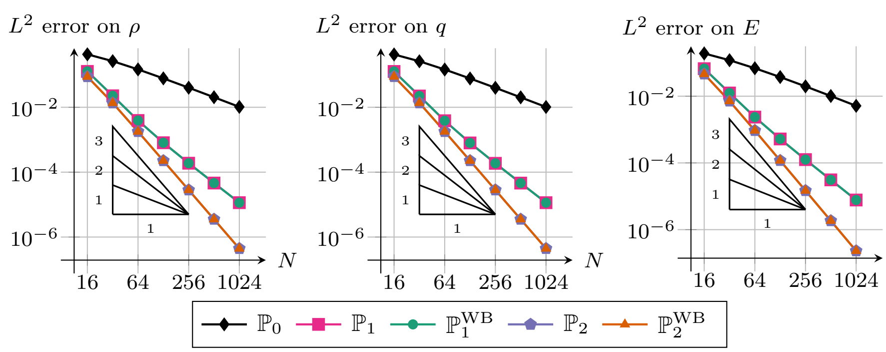

FIGURE 4. Analytical solution (5.1) with $\varphi(x) = x$: L^2 errors and EOC for the first, second and third order schemes, with or without the high-order well-balanced correction.

5.2. **Well-balanced test cases.** To numerically verify the well-balanced property of the schemes, for hydrostatic atmospheres, as well as for moving equilibria, we compute the approximations of an equilibrium at rest and a moving equilibrium.

5.2.1. *Hydrostatic equilibrium.* We begin with an isentropic hydrostatic atmosphere given by

$$
\rho_{\mathrm{hyd}}(x) = \left(1 - \frac{\gamma-1}{\gamma}\varphi(x)\right)^{1/(\gamma-1)}, \quad p_{\mathrm{hyd}}(x) = \rho(x)^\gamma, \quad u = 0. \tag{5.2}
$$

We consider the two gravitational potentials φ_1 and φ_2, on a computational domain $\Omega = [0,1]$ discretized in 50 cells. We prescribe exact boundary conditions for φ_1 and periodic boundary conditions for φ_2. In Tables 1 and 2, the L^2 errors at time t_f are compared to non-well-balanced HLL solver for φ_1 and φ_2 respectively. All well-balanced schemes are able to preserve the hydrostatic equilibrium at machine precision, whereas the HLL scheme, as expected, has a quite large error. Moreover, due to the non-trivial contribution of φ_2 the error using the HLL scheme is much higher. This underlines the necessity of well-balanced schemes.

TABLE 1. Well-balanced test case hydrostatic atmosphere with $\varphi(x) = (x-0.5)^2/2$.

	HLL	$\mathbb{P}_0$	$\mathbb{P}_1^{\mathrm{WB}}$	$\mathbb{P}_2^{\mathrm{WB}}$
ρ	$6.390 \cdot 10^{-3}$	$2.658 \cdot 10^{-15}$	$2.727 \cdot 10^{-15}$	$2.436 \cdot 10^{-15}$
q	$5.002 \cdot 10^{-4}$	$1.154 \cdot 10^{-15}$	$1.498 \cdot 10^{-15}$	$1.691 \cdot 10^{-15}$
E	$2.289 \cdot 10^{-3}$	$7.640 \cdot 10^{-15}$	$7.640 \cdot 10^{-15}$	$1.020 \cdot 10^{-14}$

TABLE 2. Well-balanced test case hydrostatic atmosphere with $\varphi(x) = \sin(x)$.

	HLL	$\mathbb{P}_0$	$\mathbb{P}_1^{\mathrm{WB}}$	$\mathbb{P}_2^{\mathrm{WB}}$
ρ	$1.109 \cdot 10^{-1}$	$3.819 \cdot 10^{-15}$	$2.620 \cdot 10^{-15}$	$4.255 \cdot 10^{-15}$
q	$1.898 \cdot 10^{-2}$	$1.439 \cdot 10^{-15}$	$1.477 \cdot 10^{-15}$	$1.522 \cdot 10^{-15}$
E	$7.170 \cdot 10^{-2}$	$7.536 \cdot 10^{-15}$	$6.822 \cdot 10^{-15}$	$7.270 \cdot 10^{-15}$

5.2.2. *Moving equilibrium.* Next, a moving equilibria is computed, characterized by the triplet $q_0 = 1$, $s_0 = 0$ and $H_0 = 5$. The gravitational potentials φ_1 and φ_2 are considered. For each φ, the initial conditions for ρ and E are obtained by solving the non-linear system (2.14) employing Newton's method. The computational domain is given by $\Omega = [0,1]$, and is partitioned in 50 cells. Homogeneous exact and periodic boundary conditions are prescribed for φ_1 and φ_2, respectively. The L^2 errors at time $t = 1$ are given in Tables 3 and 4 for φ_1 and φ_2 respectively. Similarly to the simulation of the hydrostatic atmosphere from Section 5.2.1, all well-balanced schemes are able to preserve the moving equilibrium up to machine precision, whereas the HLL scheme yields quite large errors. This verifies and illustrates the ability of the new well-balanced HLL solvers to capture moving equilibria up to machine precision, in addition to hydrostatic ones.

TABLE 3. Well-balanced test case moving equilibrium with $\varphi(x) = (x-0.5)^2/2$.

	HLL	$\mathbb{P}_0$	$\mathbb{P}_1^{\mathrm{WB}}$	$\mathbb{P}_2^{\mathrm{WB}}$
ρ	$5.569 \cdot 10^{-3}$	$3.204 \cdot 10^{-15}$	$2.897 \cdot 10^{-15}$	$2.907 \cdot 10^{-15}$
q	$1.129 \cdot 10^{-3}$	$1.916 \cdot 10^{-15}$	$1.727 \cdot 10^{-15}$	$1.803 \cdot 10^{-15}$
E	$4.188 \cdot 10^{-3}$	$7.742 \cdot 10^{-15}$	$8.970 \cdot 10^{-15}$	$6.764 \cdot 10^{-15}$

TABLE 4. Well-balanced test case moving equilibrium with $\varphi(x) = \sin(x)$.

	HLL	$\mathbb{P}_0$	$\mathbb{P}_1^{\text{WB}}$	$\mathbb{P}_2^{\text{WB}}$
ρ	$8.9233 \cdot 10^{-2}$	$2.627 \cdot 10^{-15}$	$3.607 \cdot 10^{-15}$	$4.246 \cdot 10^{-15}$
q	$2.0153 \cdot 10^{-2}$	$1.877 \cdot 10^{-15}$	$1.727 \cdot 10^{-15}$	$1.922 \cdot 10^{-15}$
E	$6.7186 \cdot 10^{-2}$	$9.930 \cdot 10^{-15}$	$9.357 \cdot 10^{-15}$	$9.607 \cdot 10^{-15}$

5.3. **Perturbation of equilibrium states.** As the main motivation behind the construction of well-balanced schemes lies in the resolution of small perturbations around equilibria, the next two sets of test cases concern the performance of the novel fully-well-balanced HLL solver on such flows. In particular, this allows the use of coarse meshes, as the solution is not polluted by background errors stemming from the resolution of the equilibrium state, which would then require a substantial grid refinement to reduce the truncation error and make the perturbation visible.

In this section, we consider the quadratic potential φ_1, and the computational domain is given by $\Omega = [0, 1]$, discretized using 50 cells, with inhomogeneous Dirichlet boundary conditions corresponding to the exact, unperturbed steady solution. For all cases, we set $C_\theta = 1$ for the $\mathbb{P}_1^{\text{WB}}$ scheme and $C_\theta = 0.15$ for the $\mathbb{P}_2^{\text{WB}}$ scheme.

5.3.1. *Perturbations of a hydrostatic equilibrium.* As a first example, we consider a perturbation around an isentropic atmosphere (5.2) taken e.g. from [14]. The initial condition is given by

$$\rho(x,0) = \rho_{\text{hyd}}(x),\ u(x,0) = 0,\ p(x,0) = p_{\text{hyd}}(x) + A \exp\left(-100\left(x - \frac{1}{2}\right)^2\right), \tag{5.3}$$

where we set the amplitudes of the perturbations to be $A = 10^{-4}$ and 10^{-12}, where the latter is of the order of the truncation error of the well-balanced solver. The difference of the numerical solution against the equilibrium $W_{\text{steady}} - W_{\text{num}}$ obtained with the novel well-balanced HLL solvers at final time $t = 0.075$ are depicted in Figure 5. The top panels contain the results with an initial perturbation of amplitude 10^{-4}, while the bottom ones display the results with the amplitude reduced to 10^{-12}. In both cases, we observe that the perturbations are clearly visible and there are no spurious artifacts from the background atmosphere.

5.3.2. *Perturbations of a moving equilibrium.* Next, a perturbation of the moving equilibrium is considered. The initial condition is given by

$$\rho(x,0) = \rho_0(x),\ q(x,0) = q_0,\ p(x,0) = p_0(x) + A \exp\left(-100\left(x - \frac{1}{2}\right)^2\right), \tag{5.4}$$

where the equilibrium states are obtained from the triplet (q_0, s_0, H_0) already introduced to build the steady solution in Section 5.2.2. The numerical results are given in Figure 6 at the final time $t = 0.075$, arranged in a similar fashion to Figure 5. The perturbation around the moving equilibrium is once again well-captured and no spurious errors are introduced from the background equilibrium. In comparison to the hydrostatic atmosphere case from Figure 5, the perturbations are skewed

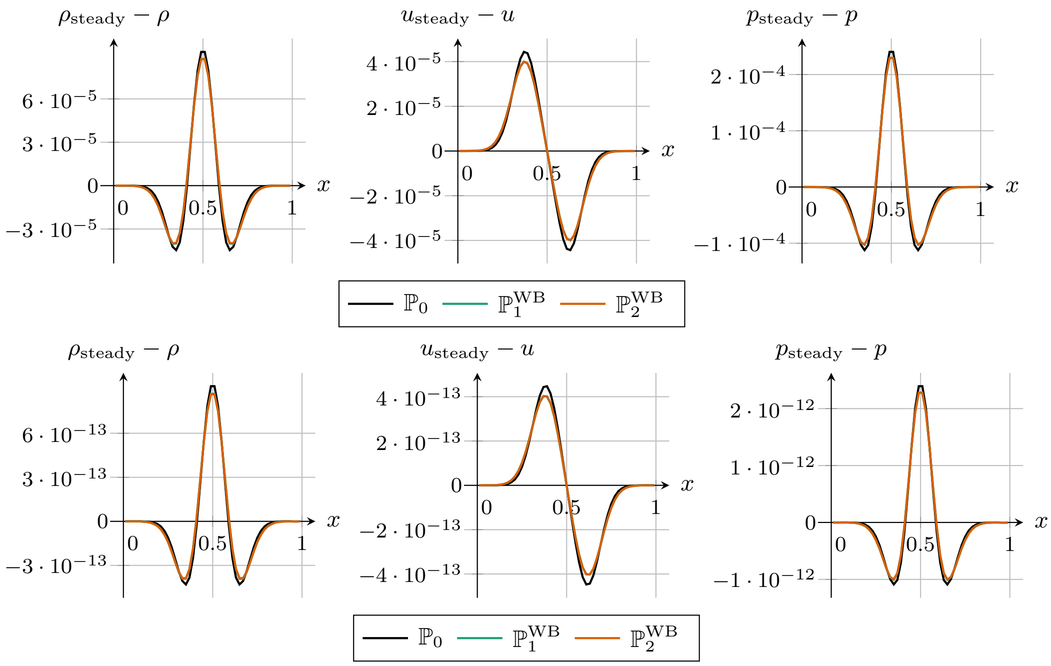

FIGURE 5. Perturbation of a hydrostatic equilibrium. Top panels: perturbation with initial amplitude $A = 10^{-4}$. Bottom: perturbation with initial amplitude $A = 10^{-12}$.

towards the right and travel faster. This is due to a non-zero positive background velocity.

Another interesting test case concerns a moving steady solution perturbed by a wave stemming from a time-dependent boundary condition. We consider again the moving equilibrium given by (q_0, s_0, H_0), with the perturbation applied as a right boundary condition acting only on the velocity, which is given at $x = 1$ and $t > 0$ by

$$u(1, t) = 10^{-8} \sin(8\pi t) \tag{5.5}$$

instead of by the unperturbed equilibrium. The computational domain is given by $[0, 1]$ using 512 cells and the simulation is stopped shortly before the perturbation reaches the opposite boundary, at $t = 0.72$. Similar set-ups can be found in [20], motivated by the study of wave propagation in stellar atmospheres. The difference between numerical results and the moving equilibrium are given in Figure 7, where we have set $\Lambda = 5$ to add some diffusion to the scheme. In this case, the perturbation remains well-resolved. The further verifies the ability of the numerical scheme to resolve small perturbations around hydrostatic and moving equilibria on coarse grids.

5.4. **Riemann Problems.** As final test cases, we consider three Riemann Problems, two classical ones without source term, and one in presence of a gravitational source term, far from an equilibrium.

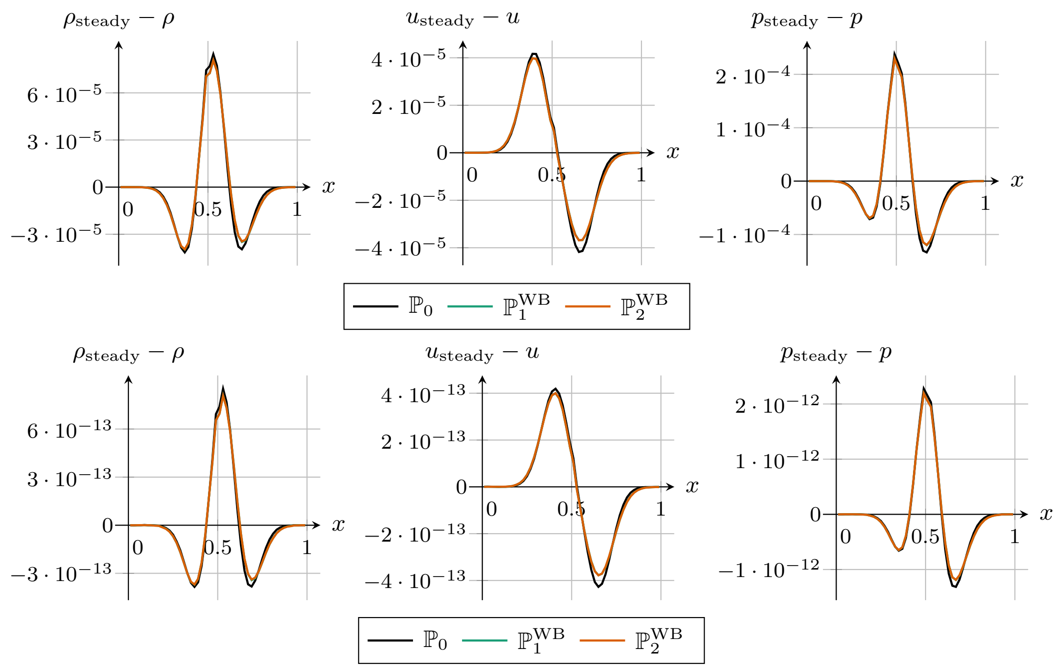

FIGURE 6. Perturbation of a moving equilibrium. Top panels: perturbation with initial amplitude $A = 10^{-4}$. Bottom: perturbation with initial amplitude $A = 10^{-12}$.

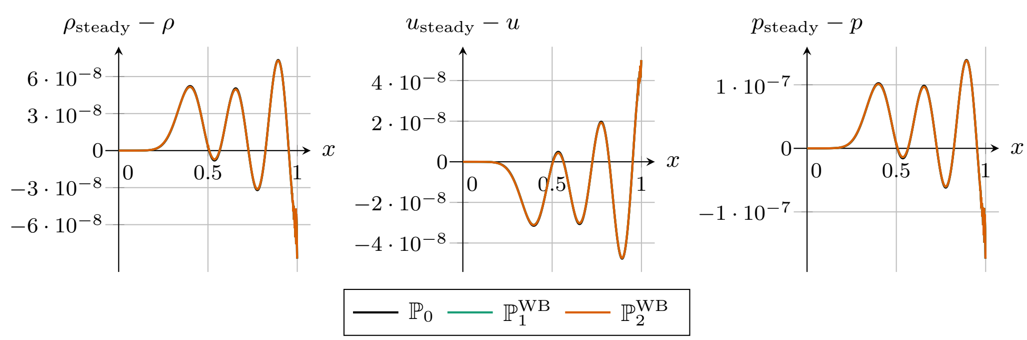

FIGURE 7. Perturbation of moving equilibrium from the boundary.

In all these cases, the space domain is $\Omega = [0, 1]$, and we prescribe homogeneous Neumann boundary conditions. Moreover, the initial condition takes the form of a Riemann problem, i.e.,

$$W(x, 0) = \begin{cases} W_L & \text{if } x < x_0, \\ W_R & \text{if } x \geq x_0, \end{cases}$$

with the jump position $x_0 = 0.5$, and where the left and right states are given differently for each problem. In each case, we take a grid consisting of 75 cells.

5.4.1. *Sod problem.* We first consider the standard Sod problem, which is a well-known benchmark for Riemann solvers. The initial condition is given by

$$\rho_L = 1, \quad \rho_R = 0.125, \quad u_L = u_R = 0, \quad p_L = 1, \quad p_R = 0.1. \tag{5.6}$$

The gravitational potential is given by $\varphi = 0$. The results are given in Figure 8, in primitive variables ρ, u and p at time $t = 0.1644$. The first order scheme is diffusive, in particular over the contact and shock waves, whereas increasing the order of the new well-balanced HLL scheme increases the resolution of all waves. As is typical for high-order schemes, small oscillations can be observed near the shock wave. However, all schemes are able to correctly determine the shock position and amplitude.

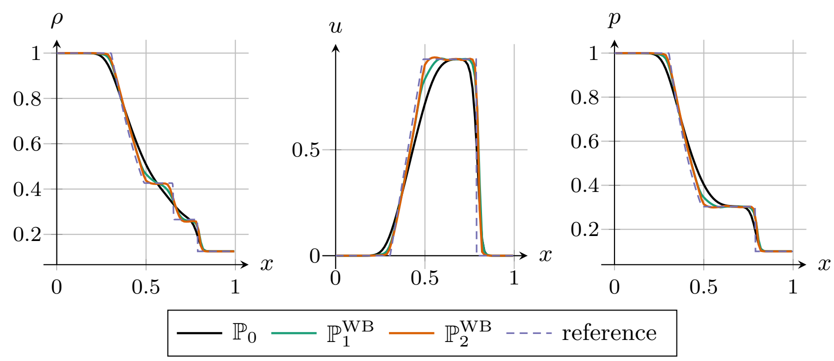

FIGURE 8. Riemann problem without a gravitational field influence: Sod problem displayed in primitive variables ρ, u and p, at time $t = 0.1644$ using 75 cells.

5.4.2. *Double rarefaction.* We then turn to a double rarefaction, whose initial data is

$$\rho_L = \rho_R = 1, \quad u_L = -\frac{10}{3}, u_R = \frac{10}{3}, \quad p_L = p_R = 1. \tag{5.7}$$

This is a challenging problem, as it will lead to a near-vacuum state in the middle of the domain. We still take the given gravitational potential $\varphi = 0$. The results are displayed in Figure 8 at time $t = 0.09$. Despite the fact that ρ and p are very close to zero in the middle of the domain, no negative values of ρ and p are observed.

5.4.3. *Riemann problem in vacuum.* The last Riemann problem is a Sod-like problem in the presence of a gravitational source term, given by φ_1. The initial data is given in steady variables q, s and H, as follows:

$$q_L = 0.5, q_R = 0, \quad s_L = 0, s_R = -\log(0.75), \quad H_L = 6, H_R = 3. \tag{5.8}$$

The results are displayed in Figure 10 at time $t = 0.2$. This time, the equilibrium variables q, s and H are displayed to underline the difference in background equilibrium. We observe that the background state is not perturbed by the new well-balanced scheme, which also accurately captures the shock and rarefaction waves.

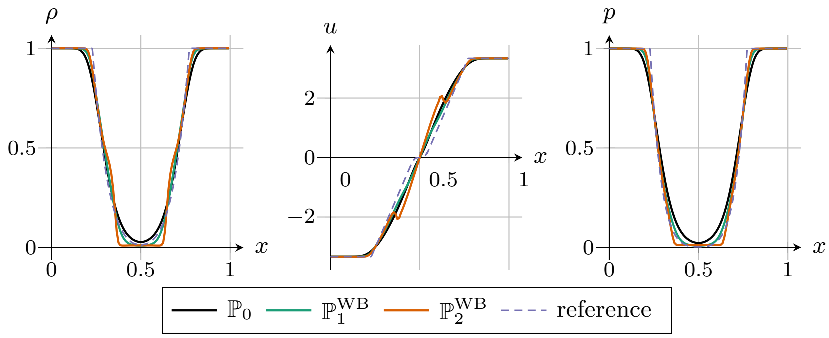

FIGURE 9. Riemann problem without a gravitational field influence: double rarefaction problem displayed in primitive variables ρ, u and p, at time $t = 0.09$ using 75 cells.

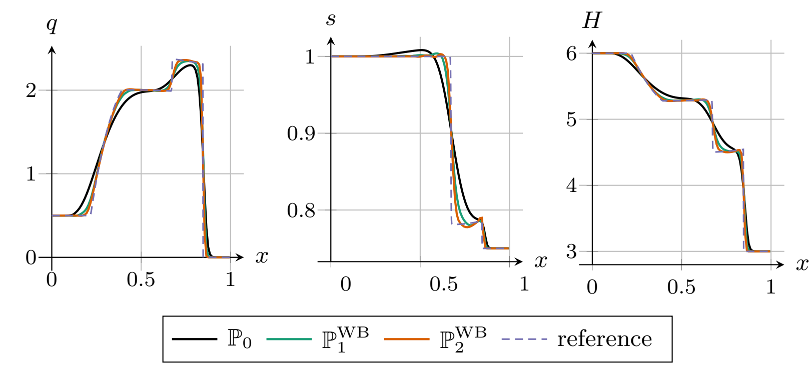

FIGURE 10. Riemann problem under a gravitational field influence: modified Sod problem displayed in steady variables q, s and H, at time $t = 0.2$ using 75 cells.

6. CONCLUSIONS

REFERENCES

1. E. Audusse, F. Bouchut, M.-O. Bristeau, R. Klein, and B. Perthame, *A fast and stable well-balanced scheme with hydrostatic reconstruction for shallow water flows*, SIAM Journal on Scientific Computing **25** (2004), no. 6, 2050–2065.
2. A. Bermudez and M. E. Vazquez, *Upwind methods for hyperbolic conservation laws with source terms*, Computers & Fluids **23** (1994), no. 8, 1049–1071.
3. C. Berthon, *Numerical approximations of the 10-moment gaussian closure*, Mathematics of Computation **75** (2006), no. 256, 1809–1832.
4. C. Berthon, S. Bulteau, F. Foucher, M. M'Baye, and V. Michel-Dansac, *A Very Easy High-Order Well-Balanced Reconstruction for Hyperbolic Systems with Source Terms*, SIAM J. Sci. Comput. **44** (2022), no. 4, A2506–A2535.
5. C. Berthon and C. Chalons, *A fully well-balanced, positive and entropy-satisfying Godunov-type method for the shallow-water equations*, Mathematics of Computation **85** (2016), no. 299, 1281–1307.
6. C. Berthon and F. Foucher, *Efficient well-balanced hydrostatic upwind schemes for shallow-water equations*, Journal of Computational Physics **231** (2012), no. 15, 4993–5015.

7. C. Berthon, M. M'Baye, M. Le, and D. Seck, *A well-defined moving steady states capturing godunov-type scheme for shallow-water model*, International Journal on Finite Volumes (2021).
8. C. Berthon and V. Michel-Dansac, *A fully well-balanced hydrodynamic reconstruction*, Journal of Numerical Mathematics (2024), no. 0.
9. F. Bouchut, *Nonlinear stability of finite volume methods for hyperbolic conservation laws and well-balanced schemes for sources*, Frontiers in Mathematics, Birkhäuser Verlag, Basel, 2004.
10. F. Bouchut and T. Morales, *A subsonic-well-balanced reconstruction scheme for shallow water flows*, SIAM Journal on Numerical Analysis **48** (2010), no. 5, 1733–1758.
11. P. Cargo and A.-Y. Le Roux, *Un schéma équilibre adapté au modèle d'atmosphère avec termes de gravité*, Comptes rendus de l'Académie des sciences. Série 1, Mathématique **318** (1994), no. 1, 73–76.
12. M. J. Castro, A. Pardo Milanés, and C. Parés, *Well-balanced numerical schemes based on a generalized hydrostatic reconstruction technique*, Mathematical Models and Methods in Applied Sciences **17** (2007), no. 12, 2055–2113.
13. C. Chalons and J.-F. Coulombel, *Relaxation approximation of the euler equations*, Journal of Mathematical Analysis and Applications **348** (2008), no. 2, 872–893.
14. P. Chandrashekar and C. Klingenberg, *A second order well-balanced finite volume scheme for Euler equations with gravity*, SIAM J. Sci. Comput. **37** (2015), no. 3, B382–B402. MR 3348134
15. G. Chen and S. Noelle, *A new hydrostatic reconstruction scheme based on subcell reconstructions*, SIAM Journal on Numerical Analysis **55** (2017), no. 2, 758–784.
16. Y. Cheng, A. Chertock, M. Herty, A. Kurganov, and T. Wu, *A new approach for designing moving-water equilibria preserving schemes for the shallow water equations*, Journal of Scientific Computing **80** (2019), no. 1, 538–554.
17. F. Coquel and B. Perthame, *Relaxation of energy and approximate Riemann solvers for general pressure laws in fluid dynamics*, SIAM Journal on Numerical Analysis **35** (1998), no. 6, 2223–2249.
18. C. M. Dafermos, *Hyperbolic conservation laws in continuum physics*, third ed., Grundlehren der Mathematischen Wissenschaften [Fundamental Principles of Mathematical Sciences], vol. 325, Springer-Verlag, Berlin, 2010. MR 2574377 (2011i:35150)
19. V. Desveaux, M. Zenk, C. Berthon, and C. Klingenberg, *A well-balanced scheme to capture non-explicit steady states in the Euler equations with gravity*, Int. J. Numer. Methods Fluids **81** (2016), no. 2, 104–127.
20. F. G. Fuchs, A. D. McMurry, S. Mishra, N. H. Risebro, and K. Waagan, *High order well-balanced finite volume schemes for simulating wave propagation in stratified magnetic atmospheres*, J. Comput. Phys. **229** (2010), no. 11, 4033–4058.
21. J. M. Gallardo, C. Parés, and M. Castro, *On a well-balanced high-order finite volume scheme for shallow water equations with topography and dry areas*, Journal of Computational Physics **227** (2007), no. 1, 574–601.
22. B. Ghitti, C. Berthon, M. Le, and E. Toro, *A fully well-balanced scheme for the 1d blood flow equations with friction source term*, Journal of Computational Physics **421** (2020), 109750.
23. E. Godlewski and P.-A. Raviart, *Hyperbolic systems of conservation laws*, Mathématiques & Applications (Paris) [Mathematics and Applications], vol. 3/4, Ellipses, Paris, 1991.
24. L. Gosse, *A well-balanced flux-vector splitting scheme designed for hyperbolic systems of conservation laws with source terms*, Computers & Mathematics with Applications **39** (2000), no. 9, 135–159.
25. J. M Greenberg and A.-Y. Leroux, *A well-balanced scheme for the numerical processing of source terms in hyperbolic equations*, SIAM Journal on Numerical Analysis **33** (1996), no. 1, 1–16.
26. L. Grosheintz-Laval and R. Käppeli, *High-order well-balanced finite volume schemes for the Euler equations with gravitation*, J. Comput. Phys. **378** (2019), 324 – 343.
27. A. Harten, P. D. Lax, and B. van Leer, *On upstream differencing and Godunov-type schemes for hyperbolic conservation laws*, SIAM Rev. **25** (1983), no. 1, 35–61. MR 693713 (85h:65188)
28. S. Jin, *A steady-state capturing method for hyperbolic systems with geometrical source terms*, ESAIM: Mathematical Modelling and Numerical Analysis **35** (2001), no. 04, 631–645.
29. S. Jin and C. D. Levermore, *Numerical schemes for hyperbolic conservation laws with stiff relaxation terms*, Journal of computational physics **126** (1996), no. 2, 449–467.
30. R. Käpelli and S. Mishra, *Well-balanced schemes for the euler equations with gravitation*, J. Comput. Phys. **259** (2014), 199–219.

31. C. Klingenberg, G. Puppo, and M. Semplice, *Arbitrary Order Finite Volume Well-Balanced Schemes for the Euler Equations with Gravity*, SIAM J. Sci. Comput. **41** (2019), no. 2, A695–A721.
32. J. Luo, K. Xu, and N. Liu, *A well-balanced symplecticity-preserving gas-kinetic scheme for hydrodynamic equations under gravitational field*, SIAM Journal on Scientific Computing **33** (2011), no. 5, 2356–2381.
33. V. Michel-Dansac, C. Berthon, S. Clain, and F. Foucher, *A well-balanced scheme for the shallow-water equations with topography*, Comput. Math. Appl. **72** (2016), no. 3, 568–593. MR 3521058
34. C. Parés and M. Castro, *On the well-balance property of Roe's method for nonconservative hyperbolic systems. Applications to shallow-water systems*, ESAIM: mathematical modelling and numerical analysis **38** (2004), no. 05, 821–852.
35. E. Tadmor, *A minimum entropy principle in the gas dynamics equations*, Appl. Numer. Math. **2** (1986), no. 3-5, 211–219. MR 863987 (88a:76037)
36. A. Thomann, M. Zenk, and C. Klingenberg, *A second-order positivity-preserving well-balanced finite volume scheme for Euler equations with gravity for arbitrary hydrostatic equilibria*, Int. J. Numer. Methods Fluids **89** (2019), no. 11, 465–482.
37. E. F. Toro, *Riemann Solvers and Numerical Methods for Fluid Dynamics* , Springer-Verlag: Berlin, 2009.
38. E.F. Toro, M. Spruce, and W. Speares, *Restoration of the contact surface in the HLL-Riemann solver*, Shock waves **4** (1994), no. 1, 25–34.
39. J. Vides, B. Braconnier, A. Audit, C. Berthon, and B. Nkonga, *A Godunov-type solver for the numerical approximation of gravitational flows*, Comm. Comput. Phys. **15** (2014), 46–75.
40. Y. Xing and C.-W. Shu, *High Order Well-Balanced WENO Scheme for the Gas Dynamics Equations Under Gravitational Fields*, J. Sci. Comput. **54** (2012), no. 2–3, 645–662.
41. K. Xu, *A well-balanced gas-kinetic scheme for the shallow-water equations with source terms*, Journal of Computational Physics **178** (2002), no. 2, 533–562.
42. K. Xu, J. Luo, and S. Chen, *A well-balanced kinetic scheme for gas dynamic equations under gravitational field*, Advances in Applied Mathematics and Mechanics **2** (2010), 200–210.

Laboratoire de Mathématiques Jean Leray, CNRS UMR 6629, Université de Nantes, 2 rue de la Houssinière, BP 92208, 44322 Nantes Cedex 3, France
Email address: christophe.berthon@univ-nantes.fr

Université de Strasbourg, CNRS, Inria, IRMA, F-67000 Strasbourg, France
Email address: victor.michel-dansac@inria.fr

Université de Strasbourg, CNRS, Inria, IRMA, F-67000 Strasbourg, France
Email address: andrea.thomann@inria.fr